13. SITE 744[1]

Shipboard Scientific Party[2]

HOLE 744A

Date occupied: 5 February 1988

Date departed: 6 February 1988

Time on hole: 1 day, 1 hr

Position: 61°34.66′S, 80°35.46′E

Bottom felt (rig floor; m, drill-pipe measurement): 2317.8

Distance between rig floor and sea level (m): 10.5

Water depth (drill-pipe measurement from sea level, m): 2307.3

Total depth (rig floor, m): 2493.9

Penetration (m): 176.1

Number of cores (including cores with no recovery): 20

Total length of cored section (m): 176.1

Total core recovered (m): 144.85

Core recovery (%): 82

Oldest sediment cored:
Depth sub-bottom (m): 176.1
Nature: nannofossil ooze
Earliest age: late Eocene
Measured velocity (km/s): 1.542

HOLE 744B

Date occupied: 6 February 1988

Date departed: 7 February 1988

Time on hole: 11 hr, 15 min

Position: 61°34.66′S, 80°35.46′E

Bottom felt (rig floor; m, drill-pipe measurement): 2317.0

Distance between rig floor and sea level (m): 10.5

Water depth (drill-pipe measurement from sea level, m): 2306.5

Total depth (rig floor, m): 2395.5

Penetration (m): 78.5

Number of cores (including cores with no recovery): 9

Total length of cored section (m): 78.5

Total core recovered (m): 79.74

Core recovery (%): 101

Oldest sediment cored:
Depth sub-bottom (m): 78.5
Nature: nannofossil ooze
Earliest age: early Miocene
Measured velocity (km/s): 1.519

HOLE 744C

Date occupied: 7 February 1988

Date departed: 7 February 1988

Time on hole: 8 hr

Position: 61°34.66′S, 80°35.46′E

Bottom felt (rig floor; m, drill-pipe measurement): 2318.5

Distance between rig floor and sea level (m): 10.5

Water depth (drill-pipe measurement from sea level, m): 2308.0

Total depth (rig floor, m): 2344.5

Penetration (m): 26.0

Number of cores (including cores with no recovery): 3

Total length of cored section (m): 26.0

Total core recovered (m): 26.77

Core recovery (%): 102

Oldest sediment cored:
Depth sub-bottom (m): 26.0
Nature: siliceous ooze
Earliest age: late Miocene
Latest age: Quaternary
Measured velocity (km/s):

Principal results: Ocean Drilling Program (ODP) Site 744 (61°34.6′S, 80°35.46′E; water depth 2307.3 m) was cored on the southern Kerguelen Plateau in order to recover a more complete Neogene and Oligocene section than that recovered at Site 738. A 176.1-m-thick uppermost Eocene to Quaternary section was cored with a composite recovery of over 95% in three holes at Site 744. The section appears to be an excellent reference section for both calcareous and siliceous microfossils as well as magnetostratigraphy for intermediate water depths in the southern Indian Ocean.

The upper 23 m of the section is uppermost Miocene to Quaternary diatomaceous ooze with a variable content of carbonate. This is separated by a hiatus that spans at least the interval from 6.1 to 8.4 Ma from at least 153 m of uppermost Eocene to upper Miocene nannofossil ooze. This nannofossil ooze contains a minor, but well-preserved, biosiliceous component in the post-Eocene part of the section.

Biostratigraphy and magnetostratigraphy indicate that the Eocene/Oligocene, Oligocene/Miocene, and possibly the Miocene/Pliocene boundaries are complete at Site 744. Hiatuses or compressed intervals occur in the middle part of the Oligocene (about 32–26 Ma), in the lower Miocene (about 22.5–19 Ma), in the middle Miocene (about 14–12 Ma), and in the upper Miocene (about 8.4–6.1 Ma). Southern Ocean microfossil zonations can be applied to the assemblages, but differences between the lowermost Oligocene diatom assemblages at Site 744 and Prydz Bay Site 739 probably reflect a paleogeographic boundary between the two areas.

The sediments at Site 744 were deposited in a pelagic setting; terrestrial influence was minimal. The presence of at least small contents of carbonate throughout indicates that the site was situated above the carbonate compensation (CCD) depth since the late Eocene, the age of oldest sediments recovered. The transition from nannofossil ooze to diatomaceous ooze may signal the northward migration of the Polar Front in the late Miocene. Note that the change toward more siliceous sediments seems to take place during

[1] Barron, J., Larsen, B., et al., 1989. *Proc. ODP, Init. Repts.*, 119: College Station, TX (Ocean Drilling Program).

[2] Shipboard Scientific Party is as given in the list of Participants preceding the contents.

the same late Miocene interval (about 7 Ma, coincident with the top of the *Denticulopsis hustedtii* Zone of diatoms) as at Site 737 on the northern Kerguelen Plateau.

Coarse sand grains and gravel chiefly of metamorphic rock types are obvious in uppermost Miocene to Quaternary sediments (to 27.2 mbsf) and less so in the lower Oligocene. These coarse fractions are thought to represent mostly ice-rafted debris, probably from Antarctica, indicating glacial conditions in the coastal areas as far back in time as earliest Oligocene.

BACKGROUND AND OBJECTIVES

When Site 738 was cored on the southern Kerguelen Plateau, the seismic record showed that the Neogene section was abnormally thin (17.75 m) at that site compared to its thickness in nearby areas (compare Fig. 4, "Site 738" chapter, this volume). An examination of French seismic line MD 47-07 also indicated that a thicker Neogene section could be obtained at target Site SKP-6B, to the northwest.

The Neogene section recovered at Site 738 contained a major unconformity between the upper Miocene and the lowermost Oligocene. This middle Cenozoic interval is an especially important time in the expansion of Antarctic glaciation (Kennett, 1978), and recovery of this interval on the southern Kerguelen Plateau was important in order to document the history of ice rafting and erosion by Circumpolar Deep Water as well as to provide a reference section for biostratigraphy and paleoclimatology. Additionally, the section should be at comparable water depths to Site 738 (about 2252 m) and nearby that site, so the two sections could form a composite middle-depth reference section for the Upper Cretaceous and Cenozoic of the southern Kerguelen Plateau. Recovery of this missing section was the primary objective at Site 744.

SITE GEOPHYSICS

A survey line (ODP line 119-09) was recorded on the approach to Site 744 using the standard geophysical gear (see "Explanatory Notes" chapter, this volume) and using Global Positioning System and Transit satellite navigation (Fig. 1). Seas were moderate during the survey. A short segment of data was recorded on the initial approach; however, the presence of more than 40 icebergs in the area prevented drilling. The ship then moved toward target Site SKP-6B to move away from heavy ice. Seismic gear was again deployed, and data were recorded across target Site SKP-6B to an intermediate location, where a continuous Neogene section was likely (Fig. 2). The beacon was dropped (shotpoint 2672), and the line was continued for about 5 min before the seismic gear was retrieved. The ship returned to the beacon to begin drilling. Because a small subsurface rise lay close to the beacon deployment point, the drilling location was shifted 200 m to the east (e.g., away from the feature and along the seismic line). The seismic results are discussed the "Seismic Stratigraphy" section (this chapter).

A sonobuoy was not deployed at this site because shallow drilling depths were anticipated and good sonobuoy velocity data existed at Site 738 for the probable soft sediments at Site 744.

OPERATIONS

Transit to Site 744

With *Maersk Master* leading the way, the ships headed north to complete the planned drilling program with two shallow sites on the southern Kerguelen Plateau. The first site to be occupied was target Site SKP-6A, about 530 km north, which had already been drilled as Site 738. A shallow penetration was planned about 3 km east of Site 738 to core an upper sediment section that was not present at Site 738.

Weather conditions became worse on 4 February, with heavy snow and rising wind. A beam swell increased to about 9 m and caused *JOIDES Resolution* to roll up to 18° (no data available from the smaller and unladen *Maersk Master*). The density of icebergs was variable, but seemed to decrease to the north. As target Site SKP-6A was approached, however, the number of icebergs increased. *Maersk Master* reached the site first, and the crew advised that 148 icebergs were within an approximately 39-km radar range.

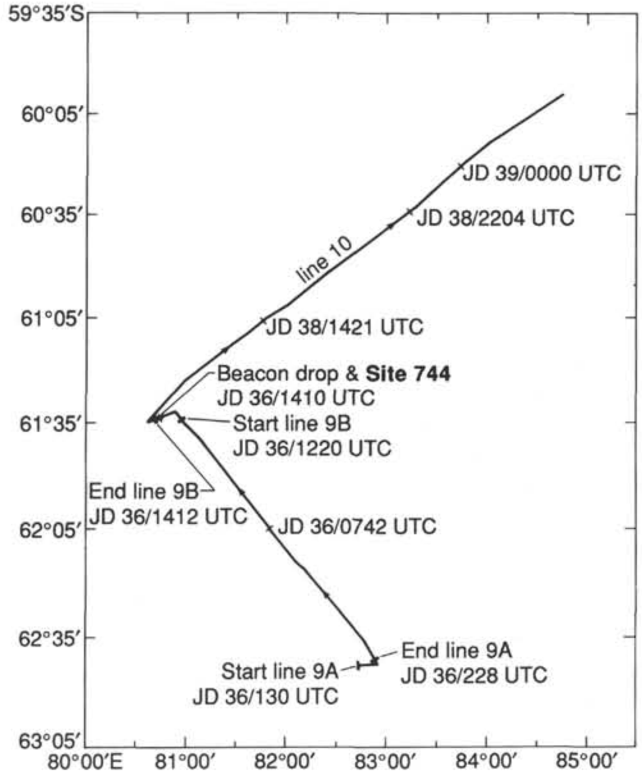

Figure 1. Index map of seismic lines recorded during site surveys for Site 744.

As the odds of completing even a relatively shallow hole without serious delays did not seem good, the approach site survey was aborted and the vessels diverted to an alternate site (SKP-6B) about 161 km northwest.

The weather improved rapidly as the little convoy approached the new site, but the icebergs were everywhere. *Maersk Master* crew again reported an unacceptable number of icebergs on and "upstream" from SKP-6B, but also noted a relatively clear area to the west and southwest of the target site. The support vessel was directed to the west and then to the northwest in the opposite direction of iceberg movement, while the drillship was moved across the target Site SKP-6B location and turned left onto a bearing of 250°. The beacon was dropped about 15 km west-southwest of the target site at a location where the geology was optimal and the ice threat was minimal. ODP management then gave us permission to drill on the adjusted coordinates.

Site 744—South Kerguelen Plateau

Hole 744A

Drilling began with the advanced piston corer (APC) at 0045 hr, 6 February 1988, establishing water depth from rig floor at 2317.8 m (see Table 1). APC coring proceeded rapidly, but core recovery was only about 60% for the first 80 m. A normal high recovery rate was then achieved to a total depth of 176.1 mbsf. APC refusal depth was not reached. After a temperature probe

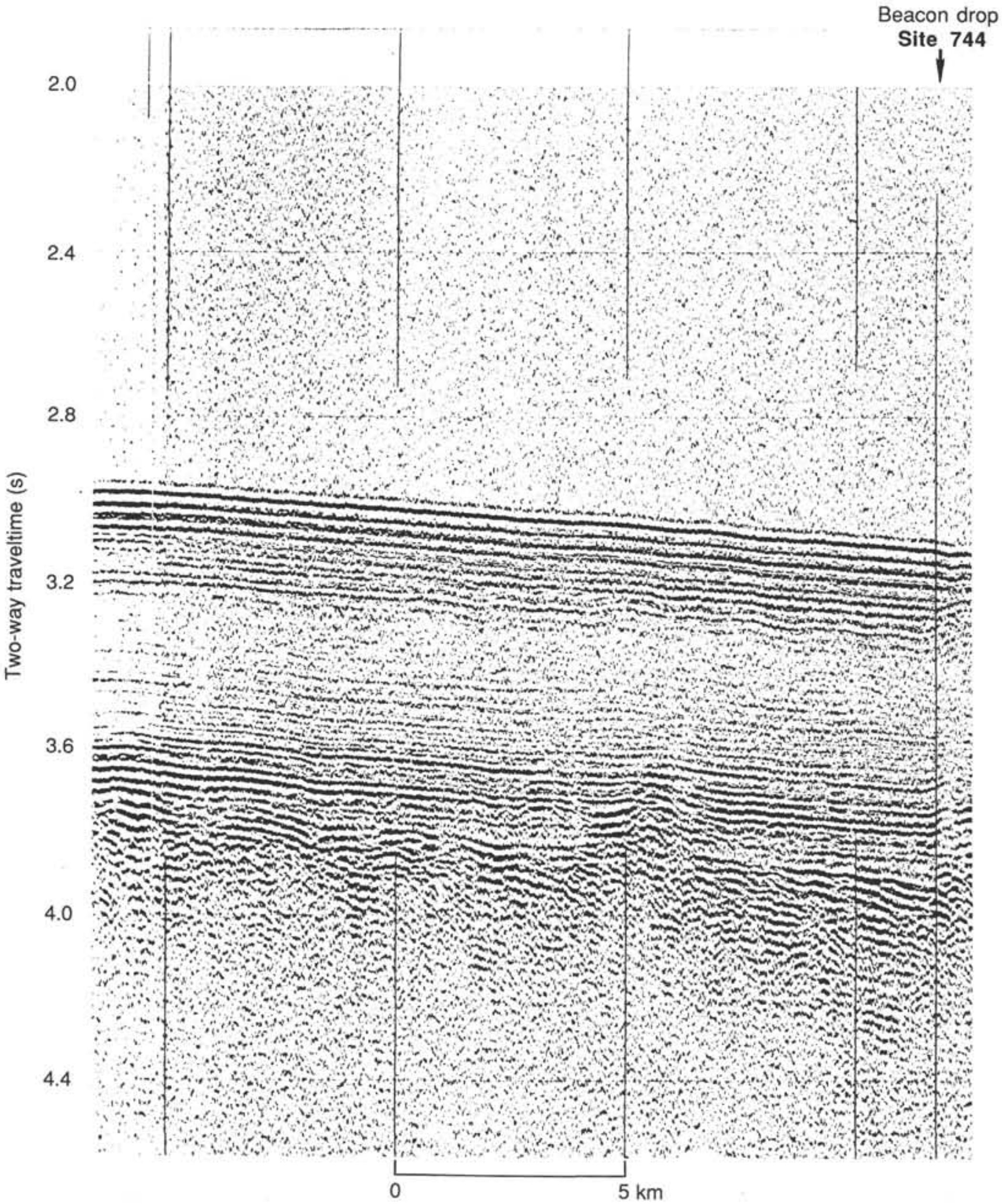

Figure 2. Seismic-reflection profile across Site 744.

run at total depth, the drill string was pulled clear of the seafloor for a second hole.

Maersk Master was released from contract duties in conjunction with drillship operations at 2400 hr because the contract, plus an extension, had expired. Ice conditions and hole depth did not warrant retention of the support vessel.

Hole 744B

The second hole was drilled to repeat the upper, incompletely recovered, interval of Hole 744A. The same coring techniques were used, except that cores were retrieved at a somewhat slower wireline speed. Complete core recovery was achieved to total depth at 79.5 mbsf. Some glacial dropstones were recovered in the shallower cores from both holes. The reduced recovery in Hole 744A may have been due either to dropstones or to turbulence at the core catcher because of high retrieval speeds. Another temperature probe measurement was taken at total depth, and the bit was again raised above the seafloor.

Hole 744C

The third hole was cored to provide dedicated cores for special scientific studies. Three APC cores were taken from the seafloor to 26 mbsf, with full recovery. The drill string then was pulled, and the vessel departed for Site 745 at 1430 hr, 7 February.

LITHOSTRATIGRAPHY AND SEDIMENTOLOGY

An almost complete sequence of upper Eocene to Quaternary sediments was drilled at Site 744 in a water depth of 2307.3 m. Core recovery was high—about 82% in Hole 744A and over 100% in Holes 744B and 744C. As a result, this site may be-

Table 1. Coring summary, Site 744.

Core no.	Date (Feb. 1988)	Time (local)	Depth (mbsf)	Length cored (m)	Length recovered (m)	Recovery (%)
119-744A-						
1H	6	0055	0.0–4.2	4.2	4.11	97.8
2H	6	0135	4.2–13.7	9.5	5.96	62.7
3H	6	0250	13.7–23.2	9.5	6.32	66.5
4H	6	0330	23.2–32.7	9.5	5.49	57.8
5H	6	0410	32.7–42.2	9.5	5.14	54.1
6H	6	0450	42.2–51.7	9.5	6.13	64.5
7H	6	0535	51.7–61.2	9.5	7.75	81.6
8H	6	0615	61.2–70.7	9.5	5.97	62.8
9H	6	0700	70.7–80.2	9.5	1.15	12.1
10H	6	0740	80.2–89.7	9.5	9.86	104.0
11H	6	0820	89.7–99.2	9.5	8.76	92.2
12H	6	0900	99.2–108.7	9.5	9.90	104.0
13H	6	0940	108.7–118.2	9.5	9.62	101.0
14H	6	1023	118.2–127.7	9.5	9.51	100.0
15H	6	1100	127.7–137.2	9.5	9.85	103.0
16H	6	1150	137.2–146.7	9.5	9.91	104.0
17H	6	1310	146.7–147.6	0.9	0.83	92.0
18H	6	1410	147.6–157.1	9.5	9.69	102.0
19H	6	1500	157.1–166.6	9.5	9.00	94.7
20H	6	1645	166.6–176.1	9.5	9.90	104.0
				176.1	144.85	82.3
119-744B-						
1H	6	2100	0.0–9.5	9.5	9.77	103.0
2H	6	2150	9.5–19.0	9.5	9.11	95.9
3H	6	2310	19.0–21.5	2.5	2.57	103.0
4H	7	0005	21.5–31.0	9.5	10.10	106.3
5H	7	0055	31.0–40.5	9.5	10.11	106.4
6H	7	0145	40.5–50.0	9.5	9.17	96.5
7H	7	0235	50.0–59.5	9.5	9.93	104.0
8H	7	0325	59.5–69.0	9.5	9.68	102.0
9H	7	0415	69.0–78.5	9.5	9.30	97.9
				78.5	79.74	101.6
119-744C-						
1H	7	0730	0.0–7.0	7.0	7.06	101.0
2H	7	0815	7.0–16.5	9.5	9.69	102.0
3H	7	0950	16.5–26.0	9.5	10.02	105.5
				26.0	26.77	102.9

come an important reference section for sedimentation in intermediate water depths in the southern Indian Ocean.

The sediments at Site 744 are characterized by a high biogenic content, which usually is >90%. The most important fossil groups are calcareous nannofossils and diatoms. Foraminifers, radiolarians, silicoflagellates, and sponge spicules only account for about 5%–20%. The sediments recovered at Site 744 can be divided into two lithologic units (Fig. 3). Unit I is dominated by a diatom ooze, and Unit II by a nannofossil ooze. All percentages of biogenic and detrital sediment components given in this chapter are based on smear slide data (Fig. 4), unless otherwise indicated. Also at this site, quartz and feldspar were difficult to distinguish in smear slides, and the two components, therefore, are best treated in combination (see "Lithostratigraphy and Sedimentology" section, "Site 739" chapter, this volume).

Drilling Disturbance

The soft nature of the sediments recovered gave rise to some drilling disturbance. Most affected were the uppermost three to five cores in each hole, which are very deformed or even soupy. Furthermore, the first section of each core typically is more disturbed than the remainder. Syringe structures in the middle of the core are typical disturbance features at this site. In general, however, the drilling disturbance was much less than in the previous few sites, due to the use of the APC. For details on the drilling disturbance see the barrel sheets.

Lithostratigraphy

Unit I

Sections 119-744A-1H-1 through 119-744A-3H-CC; depth, 0–23.2 mbsf.
Sections 119-744B-1H-1 through 119-744B-3H-CC; depth, 0–21.5 mbsf.
Sections 119-744C-1H-1 through 119-744C-3H-5, 50 cm; depth, 0–23.0 mbsf.
Age: latest Miocene to Quaternary.

Unit I consists mainly of a soft diatom ooze with fluctuating amounts of biogenic siliceous and calcareous sediment components. It is dominated by light colors: white (10YR 8/1, 10YR 8/2, 5Y 8/2, and 2.5Y 8/2), light gray (10YR 7/2), pale yellow (5Y 7/3 and 2.5Y 7/3), light yellowish brown (2.5Y 6/3), very pale brown (10YR 7/3), light olive brown (2.5Y 5/4), pale olive (5Y 6/3), and olive gray (2.5Y 4/2). The color seems to correlate with the diatom content, in that high diatom percentages generally give rise to darker colors. The sediment components are 5%–25% sand size, 70%–85% silt size, and 5%–25% clay size.

The diatom content ranges generally from 50% to 80%. Other siliceous biogenic components are much less abundant. Radiolarians normally account for 5%–15% of the sediment and silicoflagellates for up to 8%. Sponge spicules only occur sporadically, in trace amounts. The biogenic calcareous components are dominated by foraminifers, up to 20%, but normally 5%–15%. Nannofossils occur in very low concentrations (<1%), but attain 10% in Core 119-744B-2H (9.5–19.0 mbsf). Micrite is present throughout the unit except for about the lowermost 5 m. In Hole 744A the micrite concentrations are between 40% and 15%, decreasing downcore; whereas, in Holes 744B and 744C, they only account for a maximum of 10% of the sediment. The calcium carbonate profile (see "Inorganic Chemistry" section, this chapter) reflects the Hole 744A situation. The detrital component of the sediment is almost negligible. Quartz and feldspar appear only in the lower part of the unit in the silt and fine-sand fraction, and then only in small concentrations of up to 10% (quartz and feldspar). The clay content is difficult to estimate in smear slides for this type of sediment, but it is thought to be less than 10%. The concentrations of the most important sediment components are shown in Figures 4 and 5.

Coarse sand grains, granules and small pebbles up to 5 cm in diameter occur throughout the unit at <1%–2%. The clasts include quartz, lithic fragments, granite, quartz-feldspar-biotite gneiss, and amphibolite. Initial visual investigation indicated that this assemblage resembles that found in the diamictites in Prydz Bay. Most of the larger clasts are subrounded to subangular and are coated with black manganese oxide, commonly only on one side. Darker and lighter segregations are common and give the sediment a mottled appearance. Some of the mottles are clearly bioturbation features, and in some cases different generations of bioturbation can be observed.

Fluctuating concentrations of different sediment components result in a variety of minor lithologies, which are similar to diatom ooze (see barrel sheets). Only the most striking minor lithologies are mentioned here. In Section 119-744A-2H-1 (4.2–5.7 mbsf), a foraminiferal ooze contains 50% foraminifers, 25% micrite, 15% diatoms, and 10% radiolarians. It is white (10YR 8/1) to pale brown (10YR 6/3), soft, and homogeneous, except for some local mottles. Section 119-744A-2H-4 (8.7–10.2 mbsf) is a calcareous ooze that consists of 50% micrite, 20% diatoms, 15% radiolarians, and 10% foraminifers. It is pale yellow (5Y 7/3) and shows vague mottles and bioturbation, but is other-

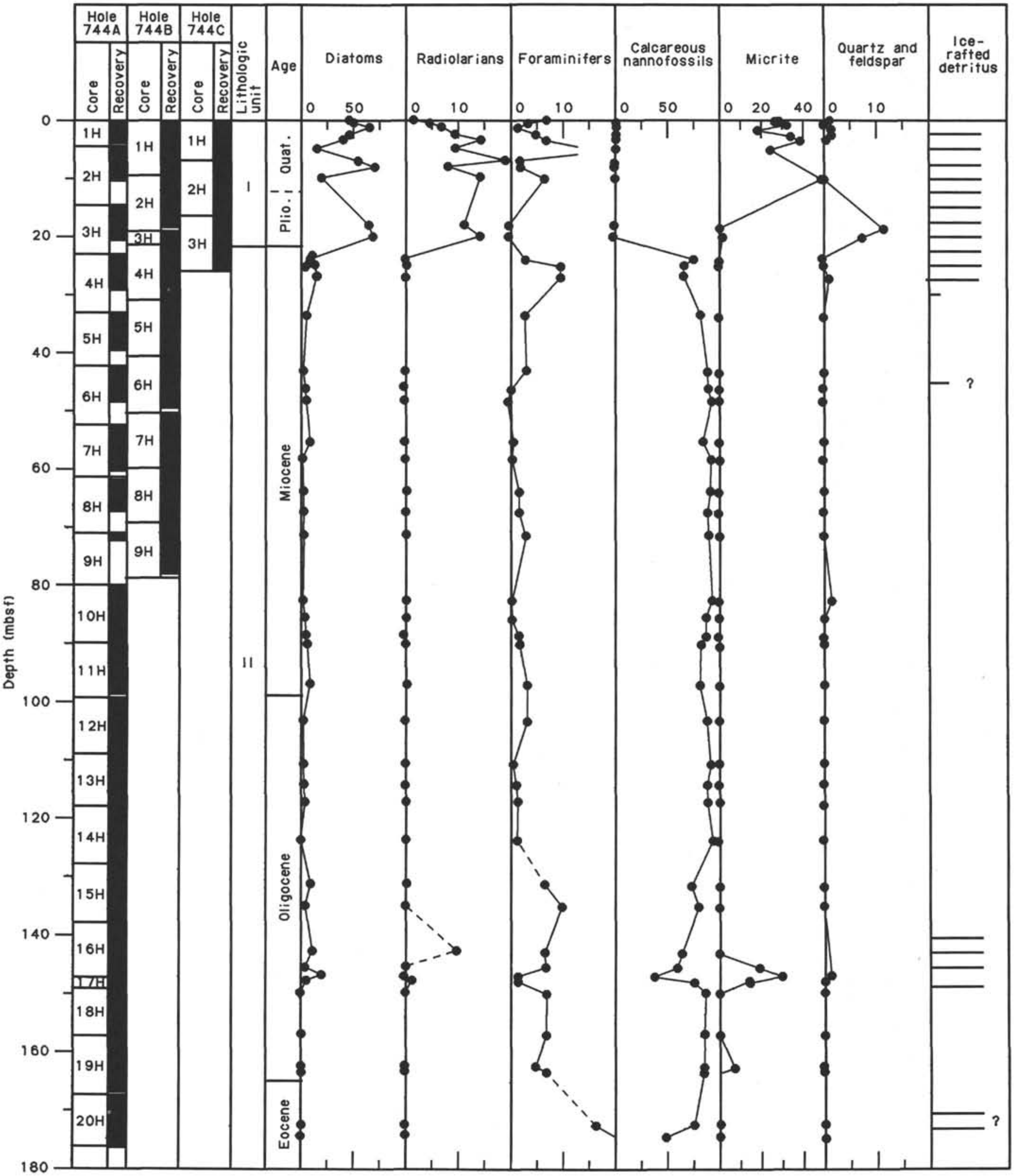

Figure 3. Summary lithologic log, Site 744.

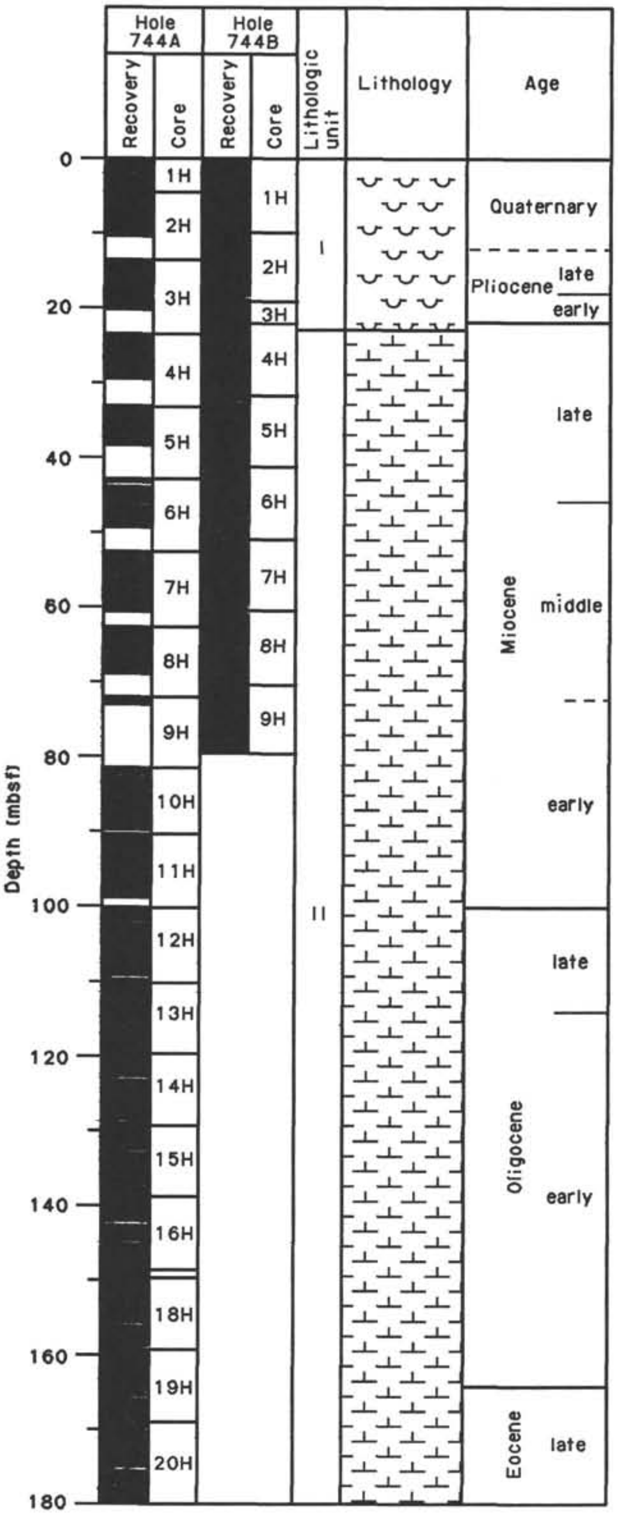

Figure 4. Summary diagram of smear slide compositional data for Site 744.

wise homogeneous and structureless. Scattered granules and small pebbles are also present. A white nannofossil ooze with about 80% nannofossils, 10%–15% diatoms, and 5% radiolarians is intercalated with the diatom ooze in Section 119-744B-3H-2, 35–75 cm.

Unit II

Sections 119-744A-4H-1 through 119-744A-20H-CC; depth, 23.2–176.1 mbsf.
Sections 119-744B-4H-1 through 119-744B-9H-CC; depth, 21.5–78.5 mbsf)
Sections 119-744C-3H-5, 50 cm, through 119-744C-3H-CC; depth, 23.0–26.0 mbsf.
Age: late Eocene to late Miocene.

Unit II is characterized by soft nannofossil ooze. Its colors are light and monotonous, although they include a large variety of different color codes: white (10YR 8/1, 10YR 8/2, 5Y 8/1, 5Y 8/2, and 2.5Y 7/2), pale yellow (2.5Y 7/3), pale gray (5Y 7/2), and light gray (10YR 7/2). Subordinate colors are gray (5Y 5/1), very pale brown (10YR 7/3), and yellow green (5GY 7/1). The slightly darker colors generally correlate with an enhanced diatom content. The sediment components of this unit are 0%–10% sand size, 50%–95% silt size, and 5%–50% clay size.

Calcareous nannofossils are the dominant component of the sediment, making up >70% and usually >85% of the sediment. In the lowermost part of the unit (below Core 119-744A-16H), they have partly disaggregated to micrite. Foraminifers are the second most abundant biogenic sediment component and occur throughout the unit. They normally range about from 3% to 5%; however, in Cores 119-744A-4H, 119-744A-15H, 119-744A-16H, 119-744A-18H, and 119-744A-19H, they reach about 10% and as high as 15%. Chemical carbonate analyses generally gave carbonate values as high as 90%, with only a few intervals where the concentrations range from 60% to 80% (see "Organic Geochemistry" section, this chapter).

High diatom contents correlate with lower nannofossil percentages. In Cores 119-744A-4H, 119-744A-5H, 119-744A-15H, and 119-744A-16H, nannofossils account for 10%–15%, while in the rest of the unit they range around 3%–5%. The other siliceous biogenic sediment components are quantitatively of no importance. Thus, radiolarians, silicoflagellates, and sponge spicules commonly are absent, or only appear as traces or a small percentage of the bulk sediment.

Nonbiogenic sediment components are also only of very minor importance in this nannofossil ooze. Clay minerals, quartz, and feldspar were identified. Quartz and feldspar occur sporadically in trace amounts or were not recognized in the smear slides because of dilution by the high biogenic supply. Only in Core 119-744A-16H do they exceed 1%. Clay seems to be present in low percentages (<5%) throughout the unit.

Scattered coarse sand grains and granules were found down to Sample 119-744A-4H-3, 100 cm (27.2 mbsf), in Hole 744A and to Section 119-744B-4H-7 (30.8 mbsf) in Hole 744B (upper Miocene). They are mostly subangular, coated with black manganese oxide, and resemble those of lithologic Unit I. One pebble of gneiss at the top of Core 119-744A-6H may have been the result of downhole contamination. Farther down the hole, black, 1- to 4-mm-diameter, manganese oxide-coated coarse sand grains are disseminated throughout Sections 119-744A-16H-7 and 119-744A-16H-CC and Cores 119-744A-17H (lower Oligocene) and 119-744A-20H (upper Eocene).

In Core 119-744A-17H, most of these coarser sand grains are concentrated along the core liner, but some others—including a 2-cm-diameter manganese oxide-coated metamorphic pebble—occur within the sediment and are clearly *in situ*. The lowermost clast of this core was found in Sample 119-744A-17H-CC, 20 cm (147.4 mbsf).

In Core 119-744A-20H, some manganese oxide-coated coarse sand grains and small granules are scattered throughout Section 119-744A-20H-1 and the upper third of Section 119-744A-20H-2. However, they may be contamination, since this part of the

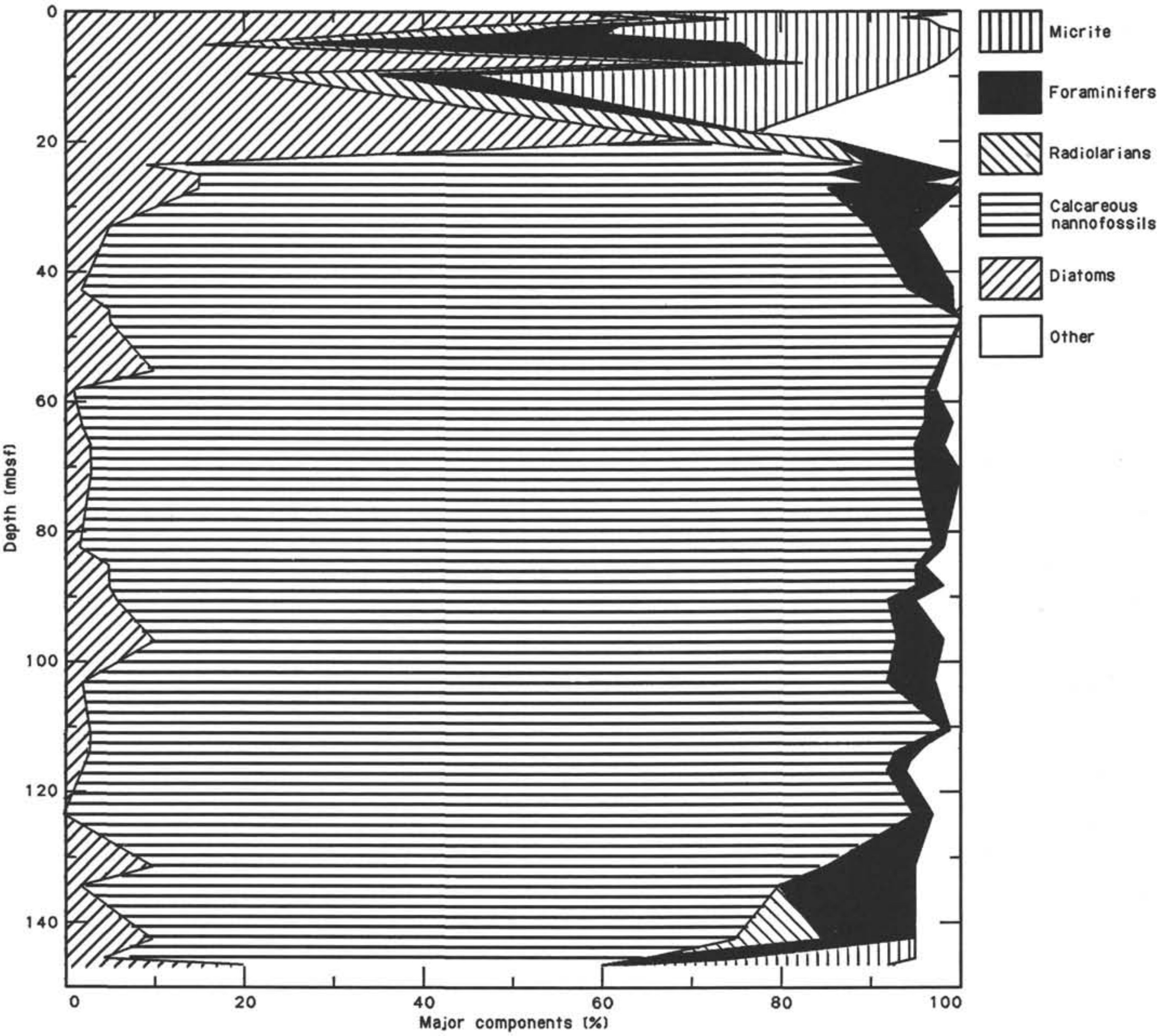

Figure 5. Abundance of the most important sediment components at Site 744. Only data from Hole 744A have been plotted. All data derived from smear slide descriptions.

core shows major drilling disturbance. The sediment is mostly soupy, and most of the clasts are "floating" in this sediment mass. The uppermost few centimeters of Section 119-744A-20H-1, 0–15 cm, however, seem undisturbed, and within the soupy interval are some relatively undisturbed sediment parts that contain rare granules. The lowermost granule was found in Sample 119-744A-20H-2, 57 cm, which is in the transition zone from the soupy to the undisturbed sediment, but which looks rather undisturbed. Section 119-744A-20H-2, 71–150 cm, has been X-rayed without finding any clasts. Thus, all the coarse fraction in this core may be due to downhole contamination.

According to the fluctuating concentrations of the individual sediment components, some minor lithologies can be described. Section 119-744A-4H-2 (24.7–26.2 mbsf) is a nannofossil ooze with minor diatoms and radiolarians. It is white (10YR 8/1), soft, homogeneous, and structureless, except for some whiter mottled patches and darker speckled (?manganese oxide-rich) streaks. In Section 119-744A-4H-3, it passes transitionally into a nannofossil ooze with minor diatoms and foraminifers, which also is mostly white (10YR 8/1), homogeneous, structureless, and has rare coarse, manganese oxide-coated grains and granules scattered throughout. In this minor lithology, paler segregations occur; the nannofossil ooze also shows a gradual change in color downcore from white to light gray (10YR 7/2). Sections 119-744A-16H-3, 10 cm, to 119-744A-16H-CC (140.3–146.7 mbsf) show a great variability in the ooze composition. This sediment consists of calcareous nannofossil ooze with minor diatoms, nannofossil ooze with minor micrite, and nannofossil calcareous ooze with minor diatoms and quartz. Finally, a white (5YR 8/1), soft, homogeneous, and structureless nannofossil ooze with minor foraminifers occurs in Sections 119-744A-20H-3, 119-744A-20H-7, and 119-744A-20H-CC (169.6–171.1 and 175.6–176.1 mbsf).

Manganese oxide streaks and fragments of submillimeter size are disseminated throughout the unit. Manganese oxide also occurs as pebbles and granules, but these are rare. Another typical feature in this lithologic unit is round or oval halo structures with diameters of up to 10 cm. They seem to be diagenetic in origin. Probably some sediment components were leached from the center, making it lighter in color. This leached material then migrated outward, precipitated out at some distance from the center (perhaps as a result of changes in the redox conditions), and formed the darker colored, diffuse ring or halo. The leached material could be manganese. Sedimentary structures generally were not observed in the nannofossil ooze, but the ooze contains common mottles of slightly darker or lighter color and diffuse bioturbation features, which could not be identified properly.

Interpretation

The sediments at Site 744 were deposited in a pelagic setting. Terrestrial influence was minimal, as indicated by the extremely low content of nonbiogenic components. Possible hiatuses were found at 26–32, 19–22.5, 12–14, and 6.1–8.4 Ma (see "Biostratigraphy" and "Sedimentation Rates" sections, this chapter). They probably are the result of strong bottom currents preventing sedimentation or removing deposited sediment.

The high carbonate content in Unit II and the presence of at least small to moderate carbonate contents in Unit I indicate that the site was situated above the CCD since late Eocene time (oldest recovered sediment). This interpretation is supported by the lack of obvious dissolution features.

Bioturbation is present throughout the core but does not seem to have been very effective or is not very obvious in the soft sediment at this site. All burrows are diffuse or only indicated by a mottled appearance of the sediment. No diagnostic features could be identified. Signs of bottom current activities are missing. The water depth during deposition of the sediments recovered might have been similar to the present one.

The transition from the nannofossil ooze of Unit II to the diatom ooze of Unit I may be explained by a northward migration of the Polar Front near the Miocene/Pliocene boundary, according to the diatom biostratigraphy (6.1–7.6 Ma). Thus, the site was beneath the high biogenic siliceous productivity zone.

Coarse sand grains and granules are obvious in Quaternary to uppermost Miocene sediments (down to Sample 119-744A-4H-3, 100 cm) and in lower Oligocene sediments (Cores 119-744A-16H and 119-744A-17H). The coarse fraction in the upper Eocene sediments (Core 119-744A-20H) probably is due to contamination. The assemblage of larger clasts in Unit I resembles that found in Prydz Bay. The composition of the smaller granules in Unit II is mostly quartz and feldspar and, thereby, also indicates an Antarctic source region. This coarse fraction of the sediments may represent ice-rafted debris. It indicates that glacial conditions were developed in eastern Antarctica or that sea ice was present as far back as early Oligocene and possibly even late Eocene time. However, a glacial input from Kerguelen Island or from western Antarctica cannot be ruled out.

BIOSTRATIGRAPHY

The highly fossiliferous uppermost Eocene through Neogene sequence recovered at Site 744 complements the previously drilled fossiliferous Turonian through lower Oligocene section of nearby Site 738. Drilled at a water depth of 2307.3 m, the sequence contains a nearly continuous representation of fossils of the two major phytoplankton (nannofossils and diatoms) and the two major zooplankton (foraminifers and radiolarians) groups. This site, therefore, provides an unique opportunity for correlation of the individual high-latitude zonations currently in use as well as for an evaluation of the changes in the supply and preservation of skeletons of the major oceanic plankton groups. Preservation of the calcareous plankton is moderate to good throughout the uppermost Eocene to Pleistocene, although their relative abundance is considerably lower in the Pliocene and Quaternary than lower in the section. This suggests a diminishing supply of calcareous skeletons during the past 5 m.y. in this subpolar area. A gradual and repeatedly interrupted rise to dominance of the siliceous plankton groups within the Upper Cenozoic was observed in the recovered sequence. Because of the high correlation between abundance and preservation in the siliceous plankton groups, no indication is yet recognizable concerning the importance of evolutionary, climatic, and preservational processes responsible for the observed pattern. More detailed shorebased analyses of this sequence, however, could provide important clues about these processes.

Calcareous Nannofossils

All core-catcher samples from Holes 744A and 744B were examined for calcareous nannofossils. Except for the first two core-catcher samples (0–19 mbsf), which contain rare to common calcareous nannofossils, all the samples yielded abundant and generally well-preserved coccoliths. For the Neogene interval, no traditional zonations can be applied for calcareous nannofossil stratigraphy, but the last-appearance datum (LAD) of *Reticulofenestra hesslandii* is useful for age assignment. It is related to the second reversal in geomagnetic Chron 5 and is at about 11.5 Ma in the time scale of Berggren et al. (1985). For the Paleogene interval, Okada and Bukry's (1980) zonation was used. Several zonal species in their scheme are rare or absent in Site 744 sediments, so some zones or subzones cannot be differentiated. Conversely, several nontraditional datum levels have been recognized and can be applied to refine the stratigraphy. The preliminary calcareous nannofossil stratigraphy results are presented in Figure 6.

Neogene

Samples 119-744A-1H-CC and 119-744A-2H-CC contain *Pseudoemiliania lacunosa,* which indicates that these samples are of early Pleistocene age or older. *Reticulofenestra perplexa* and *Reticulofenestra producta* dominate the assemblages in Samples 119-744A-3H-CC to 119-744A-6H-CC. The LAD of *R. hesslandii* was found in Sample 119-744A-7H-CC, where it is abundant. The first appearance of *Calcidiscus leptoporus* was observed between Samples 119-744A-9H-CC and 119-744B-9H-CC and defines the lower/middle Miocene boundary. The Oligocene/Miocene boundary is drawn between Samples 119-744A-11H-CC and 119-744A-12H-CC based on the occurrence of *Reticulofenestra bisecta* (few) and *Chiasmolithus altus* (abundant) in the latter sample. Rare *C. altus, R. bisecta, Reticulofenestra umbilica, Isthmolithus recurvus,* and *Zygrhablithus bijugatus* above the boundary are believed to be reworked.

Paleogene

Because neither *Sphenolithus ciperoensis* nor *Sphenolithus distentus* are present at this site, Samples 119-744A-12H-CC and 119-744A-13H-CC are assigned to the combined CP17–19 Zones in Figure 6. For the same reasons discussed in the "Biostratigraphy" section of the "Site 737" chapter (this volume), the first-appearance datum (FAD) of *Cyclicargolithus abisectus* cannot be used as a substitute for the FAD of *S. ciperoensis* as was proposed by Perch-Nielsen (1985). The interval from Samples 119-744A-14H-CC to 119-744A-19H-4, 75–76 cm, is placed in CP16. *Discoaster saipanensis* is rare at this site and was found in Sample 119-744A-19H-5, 75–76 cm. The Eocene/Oligocene boundary is therefore drawn above this sample. The FAD of *I. recurvus* falls in Sample 119-744A-20H-2, 75–76 cm, and marks the lower boundary of Subzone CP15b. The lowest interval from this hole contains *Chiasmolithus oamaruensis* but no *I. recurvus* and, therefore, falls into Subzone CP15a. In Hole 744B, which was slightly offset from the upper part of Hole 744A, the distribution of calcareous nannofossils recovered is similar.

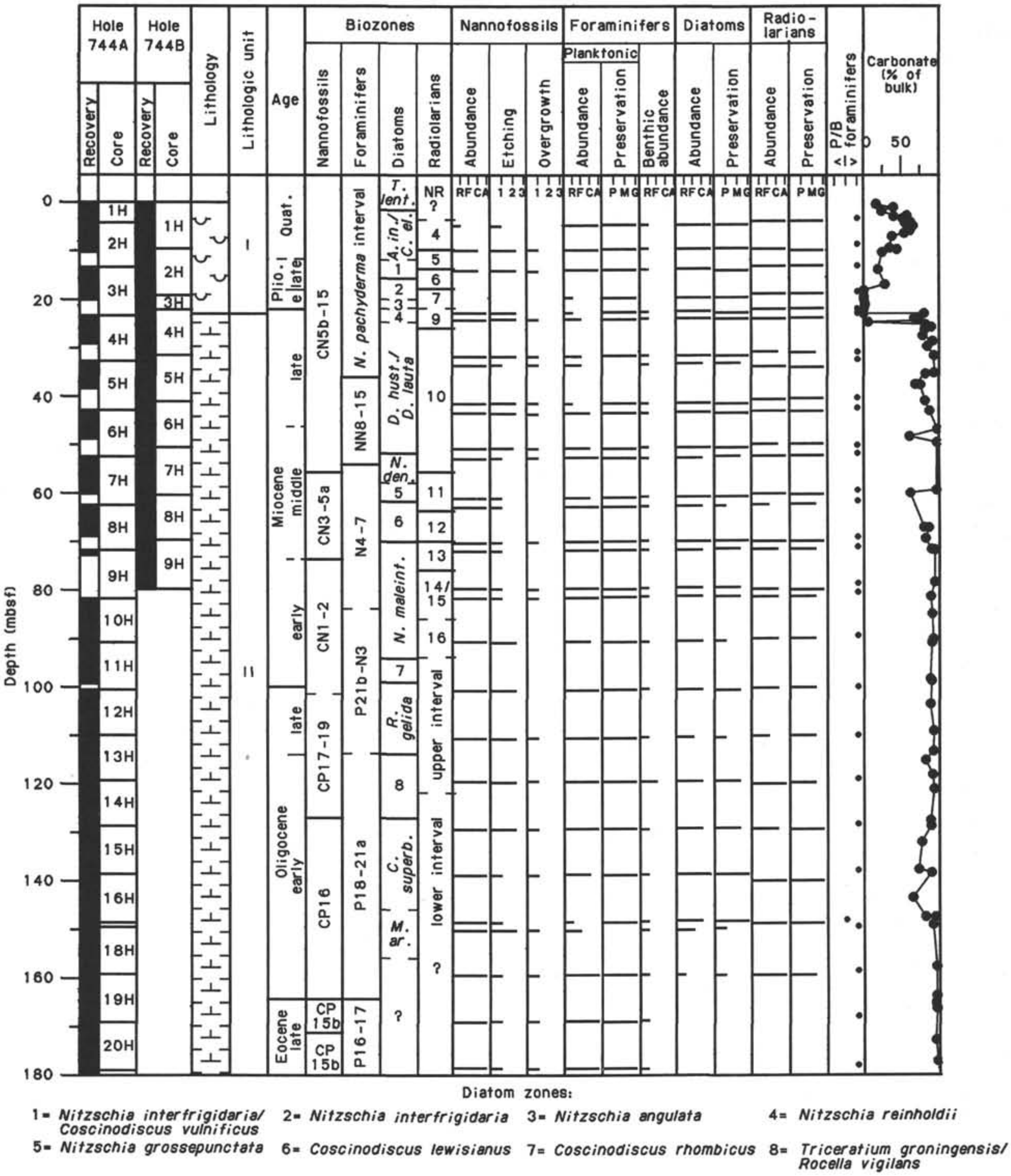

Figure 6. Biostratigraphic summary, Holes 744A and 744B.

Foraminifers

All core-catcher samples from Holes 744A and 744B were examined for foraminifers. Foraminifer abundance varies from rare to common in the biogenic siliceous intervals, which are frequent in the Quaternary and sporadic in the Miocene and older sediments, and they are abundant throughout the calcareous ooze, which dominates the Miocene and older part of the sequence. Preservation is good in all samples. Planktonic forms dominate all foraminifer assemblages except Sample 119-744A-16H-CC, which occurs in a biosiliceous interval with glacially derived dropstones. This lower Oligocene sample yields a nearly equal abundance of planktonic and benthic foraminifers.

Planktonic Foraminifers

The stratigraphic position of the foraminifer zonal boundaries shown in Figure 6, and correlation with the geochronologic time scale is approximated for Site 744 based on the recognition of planktonic foraminifer datums listed in Table 2. The stratigraphic distribution of important marker species shown in Table 3,

Table 2. Planktonic foraminifer datums at Site 744. Age determinations from the Berggren et al. (1985) time scale.

Datum[a]	Core	Chron	Age
LAD *Globorotalia zealandica*	119-744A-8H	C5D	late early Miocene (17.6 Ma)
LAD *Catapsydrax dissimilis*	119-744A-8H	C5D	late early Miocene (17.6 Ma)
FAD *Globorotalia praescitula*	119-744A-8H	C5D	late early Miocene (17.7 Ma)
LAD *Chiloguembelina cubensis*	119-744A-13H	C10	latest early Oligocene (30.0 Ma)
LAD *Globigerina angiporoides*	119-744A-14H	C11	late early Oligocene (32.0 Ma)
LAD *Globigerina ampliapertura*	119-744A-18H	C12	middle early Oligocene (32.8 Ma)
LAD *Globigerinatheka index*	119-744A-19H	C13	latest Eocene (36.6 Ma)

[a] FAD = first-appearance datum; LAD = last-appearance datum.

Table 3. Ranges in cores and age estimates of important planktonic foraminifers from Site 744.

Species	Core range	Age range
Neogloboquadrina pachyderma	119-744A-1H to -4H -744B-1H to -4H	late Miocene to Quaternary
Globigerina woodi connecta	119-744A-10H to -11H	earliest Miocene to latest Oligocene
Globigerina labiacrassata	119-744A-13H	middle Oligocene
Globigerina euapertura	119-744A-13H to -18H	early to late Oligocene
Globoborotalia opima nana	119-744A-14H to -19H	late Eocene to early Oligocene
Globigerina brevis	119-744A-15H to -19H	latest Eocene to early Oligocene
Globorotalia munda	119-744A-15H	early Oligocene
Globorotalia gemma	119-744A-15H to -19H	latest Eocene to early Oligocene
Globigerina linaperta	119-744A-18H to -20H	early to late Eocene

with correlation of planktonic foraminifer ranges from temperate to tropical sites presented by Jenkins (1985), Bolli and Saunders (1985), and Toumarkine and Luterbacher (1985). The ages for the datums in Table 2 are from the Berggren et al. (1985) geomagnetic time scale.

The upper 32 m of Holes 744A and 744B is dominated by the high-latitude assemblage of *Neogloboquadrina pachyderma, Globigerina bulloides,* and rare specimens of *Globorotalia scitula,* and is considered no older than late Miocene. Samples 119-744A-5H-CC through 119-744A-7H-CC are dominated by *Globigerina bulloides* and other globigerinids, with rare *G. scitula,* but *N. pachyderma* is absent and globorotalids are rare. This interval is considered middle to lower upper Miocene based on the absence in *N. pachyderma, Globorotalia zealandica, Globorotalia praescitula,* and *Catapsydrax* spp. The upper lower Miocene was recognized at 70.7 mbsf (Samples 119-744A-8H-CC and 119-744B-8H-CC) based on the highest occurrence of *Catapsydrax dissimilis* and *G. zealandica* and the first appearance of *G. praescitula*. The presence of *Globigerina woodi connecta* in Sample 119-744A-10H-CC, which is correlated to the *G. woodi connecta* Zone of Jenkins (1985), and the absence of that taxon and *G. zealandica* from Sample 119-744A-11H indicate that the Oligocene/Miocene boundary occurs above 99 mbsf and is probably between Cores 119-744A-10H and 119-744A-11H.

The lower Oligocene/upper Oligocene boundary was determined by the first abundant downhole occurrence of *Chiloguembelina cubensis* in Sample 119-744A-13H-CC (118.2 mbsf). Several specimens of this species were found in Sample 119-744A-12H-CC, but these were considered to be reworked. Also occurring in Sample 119-744A-13H-CC are *Globigerina labiacrassata* and *Globigerina euapertura,* which, with the absence of *Globigerinatheka index,* permit correlation with the upper part of Jenkins' (1985) *Globigerina brevis* Zone. The lower Oligocene extends down to Core 119-744A-18H, based on the presence of *Globorotalia munda* in Sample 119-744A-15H-CC and *Globorotalia gemma* in Samples 119-744A-15H-CC through 119-744A-18H-CC and the absence in these samples of *Globigerinatheka index*. The last appearance of *Globigerina ampliapertura* in Sample 119-744A-18H-CC (just above the Eocene/Oligocene boundary) is stratigraphically lower at Site 744 than reported for lower latitude locations. This earlier disappearance also occurs at Hole 738B. Furthermore, *G. ampliapertura* was reported as absent from the Maud Rise Oligocene sediments recovered during ODP Leg 113 (L. Stott, pers. comm., 1987). Thus the LAD of *G. ampliapertura,* which is reported as 32.8 Ma in low-latitude regions (Berggren et al., 1985), may have considerable latitudinal diachroneity.

The Eocene/Oligocene boundary was placed between Cores 119-744A-18H and 119-744A-19H (157.1 and 166.6 mbsf) based on the highest occurrence of *G. index* in the core-catcher sample of the latter core. *Globigerina linaperta* occurs in the core-catcher samples of both cores with *Globigerina angiporoides, Globorotalia opima nana, Globorotalia gemma,* and *Chiloguembelina cubensis*.

An upper Oligocene hiatus or condensed section was postulated for Site 744 based on the relatively small sediment thickness between the lowest occurrence of *G. woodi connecta* (Oligocene/Miocene boundary; 80.2–89.7 mbsf) and the LAD of *C. cubensis* (30 Ma; 109–118 mbsf). The sediment thickness that separates the LAD of *C. cubensis* and LAD of *G. angiporoides* (32 Ma; 118.2–127.7 mbsf) in the upper lower Oligocene is small in comparison to the 2-m.y. gap that separates these datum events. This indicates that a hiatus or an interval of diminished sediment-accumulation rate occurs in the upper lower Oligocene.

Benthic Foraminifers

Benthic foraminifers were studied from the mud-line sample and all core-catcher samples recovered from Holes 744A and 744B. Benthic species are rare compared to planktonic microfossils throughout the sequence, but abundance is sufficient to perform a quantitative study. Preservation is moderate to good. The benthic fauna in all samples examined is predominantly calcareous, with few specimens and species of agglutinated forms. The benthic assemblage shows a relatively high species diversity throughout the entire cored sequence. The benthic fauna was subdivided into the following assemblages.

Assemblage 1 (Quaternary to upper upper Miocene)

Assembly 1 ranges downcore to Core 119-744A-4H. The mud-line sample yields rare agglutinated specimens of *Reophax dentaliniformis, Rhabdammina* sp., *Cribrostomoides wiesneri,* and *Lagenammina laguncula*. The calcareous component is represented by *Cibicidoides* sp., *Epistominella exigua, Melonis pompilioides, Pullenia quinqueloba, Pullenia simplex,* and *Fursenkoina* sp. Farther down in the section the fauna is dominated by *E. exigua,* corresponding with Site 738 for the Pliocene/Quaternary interval. This species is associated with the Circumpolar Deep Water (see "Biostratigraphy" section, "Site 738" chapter, this volume). Additional Pliocene species include *Globocassidulina subglobosa, Quinqueloculina seminula, Pyrgo murrhina, Eggerella bradyi,* and *Pullenia bulloides*. In the upper Miocene an increase in diversity was found with taxa such as *Laticarinina pauperata, Stilostomella* spp., *Oridorsalis umbonatus, Uvigerina* spp., *Gyroidinoides* spp., *Pleurostomella acuta,* and *Nonion havanensis*.

Assemblage 2 (middle upper Miocene to middle Oligocene)

Cores 119-744A-5H through 119-744A-7H (middle to upper Miocene) are characterized by an impoverished benthic fauna with low species diversity. Remaining species include *P. bulloides*, *E. bradyi*, *N. havanensis*, and *Stilostomella* spp. *Karreriella cubensis* occurs in Sample 119-744A-5H-CC. The upper boundary of assemblage 2 is placed at the last occurrence of *Nuttalides umbonifera*, a species that ranges throughout most of the interval, with its first appearance in the middle lower Oligocene (Sample 119-744A-15H-CC) and its last appearance in the upper Miocene (Sample 119-744A-5H-CC). *N. umbonifera* increases in abundance upsequence and dominates in the middle upper Miocene. This range compares with the occurrence of this species in the southwestern Pacific (Deep Sea Drilling Project [DSDP] Leg 90), where the species is dominant in the upper Miocene and is interpreted as an indicator of cooling in bottom-water temperature and the influence of Antarctic Bottom Water (Kurihara and Kennett, 1985). Lower Miocene–upper Oligocene sediments (Cores 119-744A-8H to 119-744A-11H) are characterized by an increased species diversity. Additional taxa, such as *Cibicidoides praemundulus*, *Bulimina alazanensis*, and *Amphicoryna hirsuta*, are included in this assemblage. The middle Oligocene sequence (Cores 119-744A-12H to 119-744A-17H) is characterized by the presence of *Orthomorphina havanensis*, with its last appearance in Core 119-744A-12H. Other species diagnostic of this interval include *Heronallenina* sp., *Bolivina antegressa*, and *Karreriella subglabra*.

Assemblage 3 (lower Oligocene to upper Eocene)

The upper boundary of assemblage 3 was placed at the last occurrence of *Spiroplectammina spectabilis*, *Bolivinopsis* sp., *Osangularia mexicana*, and *Cibicidoides laurisae*. Additional species include *Oridorsalis umbonatus*, *Orthomorphina havanensis*, *Stilostomella* spp., *Cibicidoides ungerianus*, and *Pleurostomella acuta*. This species composition resembles assemblage 3 at Site 738. *Nuttalides truempyi*, an important marker for the Paleocene and Eocene, was not found at Site 744 in the uppermost Eocene.

Comparison of Faunas at Sites 738 and 744

A comparison of the upper three benthic assemblages at Sites 738 and 744, both located on the southern Kerguelen Plateau in similar water depths, show additional information about their development. A well-preserved upper Oligocene–Miocene sequence that was recovered from Hole 744A is absent from Site 738 due to a hiatus. This large hiatus prevents recognition of several intervals among the assemblages at both sites. The Pliocene/Quaternary sequence of assemblage 1 occurs at both sites and is dominated by *Epistominella exigua*. Assemblage 2 at Site 744, dominated by *Nuttalides umbonifera*, is completely absent from Site 738 because of the unconformity. Assemblage 3 at Site 744 contains components of assemblages 2 and 3 at Site 738. The species composition is comparable, although the dominances and diversity vary.

Bathyal benthic foraminifers are known for their slow evolution, resulting in long stratigraphic ranges. Many of these long-ranging species were found in this material, and their exact first and last appearances should be examined in a shorebased high-resolution study with more detailed taxonomy. Boltovskoy (1978) stated that the Holocene fauna developed no later than the Oligocene and, for several species, possibly in the Eocene. No faunal change was observed across the Oligocene/Lower Miocene boundary in DSDP sites along Ninteyeast Ridge (Boltovskoy, 1978). This would correspond with the observed long range of assemblage 2 from the middle Oligocene to upper Miocene at Site 744. A faunal turnover in the middle Miocene was observed in the Atlantic Ocean by Schnitker (1979) and Berggren (1972) and in the Pacific Ocean by Douglas (1973). At Site 744, a change in the benthic fauna was recognized somewhat later in the upper Miocene.

Diatoms

Diatoms are generally common to abundant and well preserved in the Oligocene to Quaternary section at Site 744. The lowermost Oligocene sample, 119-744A-18H-CC, contains only sparse, poorly preserved diatoms; underlying Samples 119-744A-19H-CC and 119-744A-20H-CC are barren of diatoms. Southern Ocean diatom zonations are readily applicable, although parts of the lower Miocene and the uppermost Miocene can be zoned by low-latitude diatom biostratigraphy.

Sample 119-744A-1H-1, 8 cm, was assigned to the *Thalassiosira lentiginosa* Zone. However, the core-catcher samples from the first cores of Holes 744A, 744B, and 744C were placed in the *Coscinodiscus elliptipora/Actinocyclus ingens* Zone, as was Sample 119-744A-2H-2, 150 cm.

Upper Pliocene samples include 119-744A-2H-CC (*Cosmiodiscus insignis* Zone?); 119-744A-2H-3, 50 cm (*Nitzschia interfrigidaria/Coscinodiscus vulnificus* Zone); and 119-744A-3H-2, 33 cm (*Nitzschia interfrigidaria* Zone).

Species characteristic of the lower Pliocene *Nitzschia angulata* Zone are in Samples 119-744B-3H-CC and 119-744C-3H-1, 133 cm. Samples 119-744A-2-CC and 119-744C-3H-2, 40 cm, through 119-744C-3H-3, 60 cm, were assigned to the uppermost part of the *Nitzschia reinholdii* Zone above the first occurrence of *Thalassiosira gracilis* (about 4.8 Ma).

As at nearby Site 738, a thin interval of uppermost Miocene sediment is characterized by the presence of *Thalassiosira miocenica* (Samples 119-744B-4H-1, 70 cm, 119-744B-4H-2, 24 cm, 119-744C-3H-3, 90 cm, and 119-744C-3H-4, 98 cm). This thin interval (2.7 m thick in Hole 744B) contains abundant reworked *Denticulopsis hustedtii* and *Actinocyclus ingens* from the underlying lower upper Miocene, and its contact with this underlying interval is marked by a distinct color change from brown above to cream below at about 47 cm in Section 119-744B-3H-5. This contact appears to be a hiatus spanning at least the interval from 6.1 to 8.4 Ma.

The lower upper Miocene *Denticulopsis hustedtii* Zone is apparently removed at a hiatus. Samples 119-744B-4H-2, 90 cm, 119-744B-4H-CC, 119-744A-4H-1, 40 cm, 119-744A-4H-CC, 119-744A-5H-CC, 119-744B-5H-CC, and 119-744B-6H-CC were placed in the *D. hustedtii/D. lauta* Zone, which spans the middle Miocene/upper Miocene boundary.

The *Nitzschia denticuloides* Zone is represented by Samples 119-744A-6H-CC and 119-744B-7H-3, 70–72 cm, and it may be separated by an unconformity or compressed interval from the underlying early middle Miocene *Nitzschia grossepunctata* Zone (or its equivalent *Denticulopsis hyalina* Zone) in Samples 119-744A-7H-CC, 119-744B-7H-6, 70–72 cm, 119-744B-7H-CC, and 119-744B-8H-CC.

The presence of *Nitzschia malinterpretaria* in Samples 119-744A-9H-CC, 119-744A-10H-CC, 119-744B-9H-1, 58–60 cm, and 119-744B-9H-CC places these samples into the combined *N. interpretaria–Coscinodiscus rhombicus* Zones of the upper lower Miocene. The absence of *C. rhombicus* in at least the latter sample is considered to be due to ecological exclusion, and whether this species is a good stratigraphic marker for the Southern Ocean is unclear.

The lowermost Miocene to uppermost Oligocene *Rocella gelida* Zone is represented by Samples 119-744A-11H-CC and 119-744A-12H-CC. The latter sample is considered to be lowermost Miocene, based on the presence of *Rocella gelida* var. *schraderi* and *Thalassiosira spinosa* (Barron, 1983).

Sample 119-744A-13H-CC contains *Synedra jouseana*, *Pyxilla reticulata*, and *Kozloviella minor* and is assigned to the *K. minor* Zone of Gombos and Ciesielski (1983). Underlying Samples 119-744A-14H-CC and 119-744A-15H-CC have diatom assemblages characteristic of Gombos and Ciesielski's (1983) *Coscinodiscus superbus* Zone (lower Oligocene). Sample 119-744A-16H-CC is assigned to the *Melosira architecturalis* Zone of Gombos and Ciesielski (1983) based on the presence of *M. architecturalis* and *Rhizosolenia gravida*. If the absence of *R. gravida* in Sample 119-744A-17H-CC is not due to ecological exclusion, then that sample could be correlated with the lowermost Oligocene *Asterolampra insignis* Zone of Gombos and Ciesielski (1983).

Note that the lower Oligocene diatom assemblage of Site 744 differs from that of Prydz Bay Site 739 in that it commonly contains *Coscinodiscus superbus* and *Rhizosolenia gravida* and lacks many of the *Stephanopyxis* species found in the lower Oligocene of Site 739.

Radiolarians

Radiolarians are consistently present and well preserved in Oligocene to Pleistocene sediments. Upper Eocene and lowermost Oligocene sediments are barren of radiolarians.

Sample 119-744A-1H-CC contains an abundant and well-preserved assemblage dominated by *Theocalyptra davisiana, Antarctissa ewingi,* and *Antarctissa strelkovi*. The diversity of the species population is high. This assemblage correlates with the lower Pleistocene NR4 Zone (Fig. 6), because it includes rare specimens of *Antarctissa denticulata, Phormostichoartus pitomorphus*, and no *Clathrocyclas bicornis* representatives. Sample 119-744A-2H-CC was assigned to the upper Pliocene NR5 Zone because of the abundance of *Clathrocyclas bicornis* and *A. ewingi*. Some rare specimens of *T. davisiana* indicate an age younger than 2.5/2.6 Ma. Sample 119-744A-3H-CC contains a well-preserved assemblage with *C. bicornis, A. ewingi, Helotholus praevema, Prunopyle titan, Desmospyris rhodospyroides, Triceraspyris coronata,* and *Lychnocanium grande* (many silicoflagellates were observed). The occurrence of some specimens of *Stichocorys peregrina* correlates this assemblage to the NR9 Zone (upper Miocene to lower Pliocene).

Samples 119-744A-4H-CC and 119-744A-5H-CC have an abundant and well-preserved population. Species such as *Clathrocyclas bicornis spongothorax, Desmospyris rhodospyroides,* and *Actinomma tanyacantha* are diagnostic of the NR10 Zone (upper Miocene). Representatives of *S. peregrina* were not found. The few temperate species found, such as *Phormostichoartus fistula* and *Clathrocyclas cabrilloensis*, indicate a warmer environment occurred in the lower part of the interval.

The abundance of *Botryopera conradae,* and the small number of *C. b. spongothorax* place Sample 119-744A-6H-CC in the lower NR10 Zone (middle Miocene to upper Miocene). Radiolarians are less abundant and moderately preserved in Sample 119-744A-7H-CC. Robust forms such as *Stichopodium cienkowski, Prunopyle hayesi,* and *Cyrtocapsella tetrapera* are predominant. The absence of many stratigraphic markers does not permit a more precise age assignment than early Miocene to this sample. Preservation of radiolarians is better in Sample 119-744A-8H-CC. Species such as *Clathrocyclas golli, Clathrocyclas regipileus, Cyrtocapsella isopera, Eucyrtidium(?) punctatum,* and *Spongomelissa dilli* are diagnostic of the NR13 Zone (lower Miocene).

Sample 119-744A-9H-CC cannot be related to a precise zone because many stratigraphic markers are missing. Sample 119-744A-10H-CC is tentatively correlated to the NR16 Zone because it contains the first occurrence of *C. tetrapera,* diagnostic of the lower Miocene. Other species, such as *C. golli, Lithocarpium frakesi,* and *P. hayesi,* are rare. Many corroded spumellarians and orosphaerids indicate strong dissolution of the radiolarian assemblage. Sample 119-744A-11H-CC was tentatively placed in the upper Oligocene because no *C. tetrapera* were found. Samples 119-744A-12H-CC and 119-744A-13H-CC present the same radiolarian assemblage as Sample 119-744A-11H-CC. The last occurrence of the *Cyclampterium milowi* group (= *C. longiventer* Chen) is located in Sample 119-744A-13H-CC. (Many silicoflagellates found here, such as *Corbisema arkhangelskia, Mesocena apiculata,* and *Cannopilus major*, are indicative of a late Oligocene age [Perch-Nielsen, 1985].) Samples 119-744A-14H-CC through 119-744A-18H-CC are of an early Oligocene age because the radiolarian assemblages contain an increasing proportion of late Eocene species, such as *Periphaena decora, Siphocampe eocenica, Stylosphaera coronata* gr., *Lithomitrella* sp., and *Calocyclas asperum*. Many ebridians and silicoflagellates, such as *Naviculopsis biaperculata, Mesocena oamaruensis,* and *Cannopilus hemisphaericus* can also be recognized. Preservation is good down to Sample 119-744A-17H-CC, but very poor in Sample 119-744A-18H-CC, where many empty shells of spumellarians indicate strong dissolution. Silicoflagellates are absent. As Samples 119-744A-19H-CC and 119-744A-20H-CC are barren of radiolarians, no Eocene/Oligocene boundary could be identified.

Radiolarian biozones determined from the core-catcher samples of Hole 744B are comparable to those observed in Hole 744A and show that an almost continuous sequence of Oligocene to Pleistocene age was drilled at Site 744 (see Fig. 6). Sample 119-744B-1H-CC contains an early Pleistocene assemblage related to the NR4 Zone. Stratigraphical markers, such as *Desmospyris spongiosa, Prunopyle titan,* and *Pseudocubus vema,* diagnostic of a late early Pliocene age, are abundant in Sample 119-744B-2H-CC, which can be related to the NR6 Zone. A well-preserved and abundant population was recognized in Sample 119-744B-3H-CC. Abundant *Helotholus praevema, P. titan, Triceraspyris coronata,* and *D. spongiosa* are diagnostic of the NR7 Zone (lower Pliocene). Samples 119-744B-2H-CC and 119-744B-3H-CC correspond to Samples 119-744A-2H-CC (NR5 Zone) and 119-744A-3H-CC (NR9 Zone).

The absence of Zone NR8 in the core-catcher samples from both holes is not indicative of a hiatus because the Pliocene sedimentation appears to be very condensed at Site 744. Radiolarian populations observed in Samples 119-744B-4H-CC to 119-744B-6H-CC are similar to those described in Samples 119-744A-4H-CC to 119-744A-6H-CC (NR10). The presence of the rare species *Thyrsocyrtis clausa* in Sample 119-744B-7H-CC is indicative of the NR11 Zone (middle Miocene). Sample 119-744B-8H-CC is correlated to the NR12 Zone because of the absence of *Actiomma tanyacantha* and the abundance of *Botryopera conradae*. Sample 119-744B-9H-CC is tentatively placed in the NR13/14 Zones (lower Miocene) because no *Spongomelissa dilli* were observed.

Palynomorphs

No palynomorphs were observed in the core-catcher samples from Site 744.

PALEOMAGNETICS

Paleomagnetic studies were completed on samples and cores from the three holes drilled at Site 744. Archive halves of the sedimentary cores (Cores 119-744A-1H through 119-744A-20H and 119-744B-1H through 119-744B-9H) were measured on the cryogenic magnetometer aboard ship. Discrete oriented samples were collected from both Holes 744A (168 oriented cubes) and 744B (139 oriented cubes). These samples were then measured on the cryogenic magnetometer. The upper portion of the sedimentary sequence from the seafloor to approximately 80 mbsf was repeated in both Holes 744A and 744B. The sedimentary sequence from Hole 744C was measured for core repository tests and will not be discussed as part of this report. The polarity reversal sequence reported is a composite of the results from

Holes 744A and 744B. No demagnetization studies were done on these sediments.

The reversal stratigraphy found within these holes correlates well with standard geomagnetic reversal sequences (Berggren et al., 1985). The sequence of reversals defined on the basis of the cryogenic magnetometer measurements of archive halves (after demagnetization to 5 and 9 mT) are shown in Figure 7. A lengthy series of polarity changes was observed and the indicated correlations are summarized in Figure 8. The youngest po-

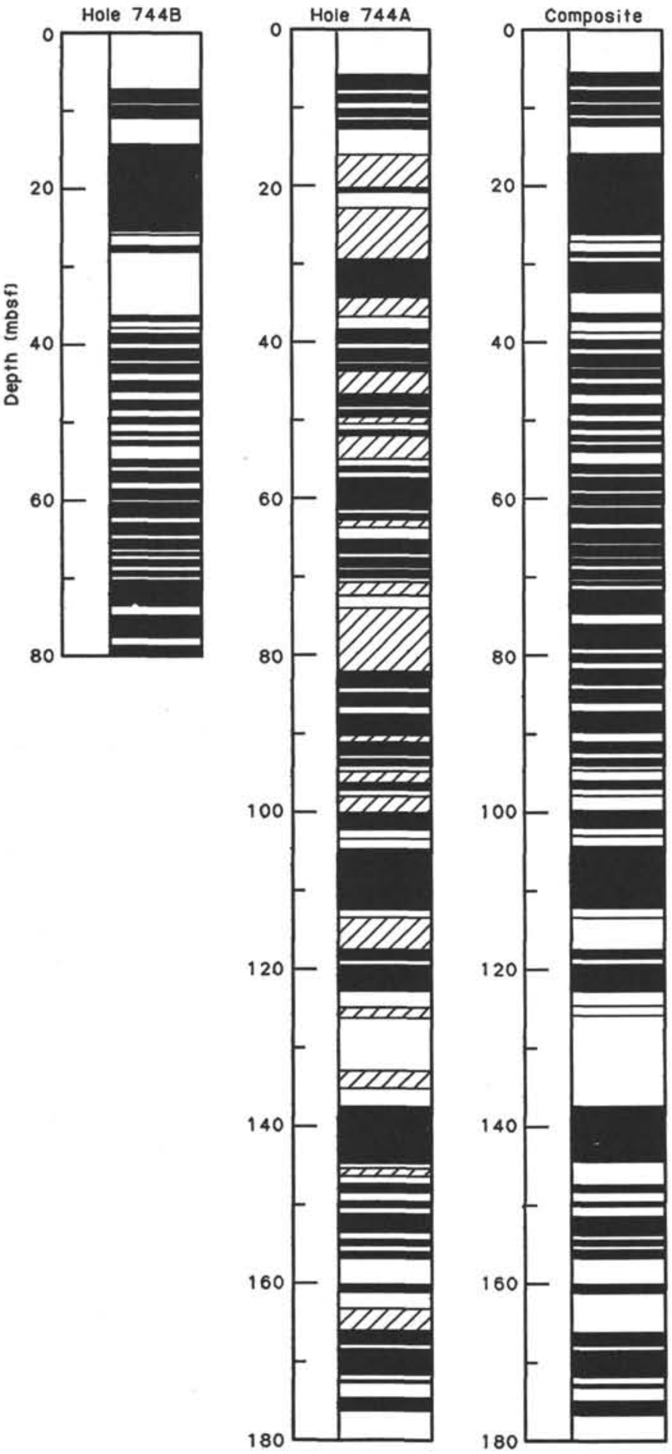

Figure 7. Magnetic polarity sequences from Holes 744A and 744B.

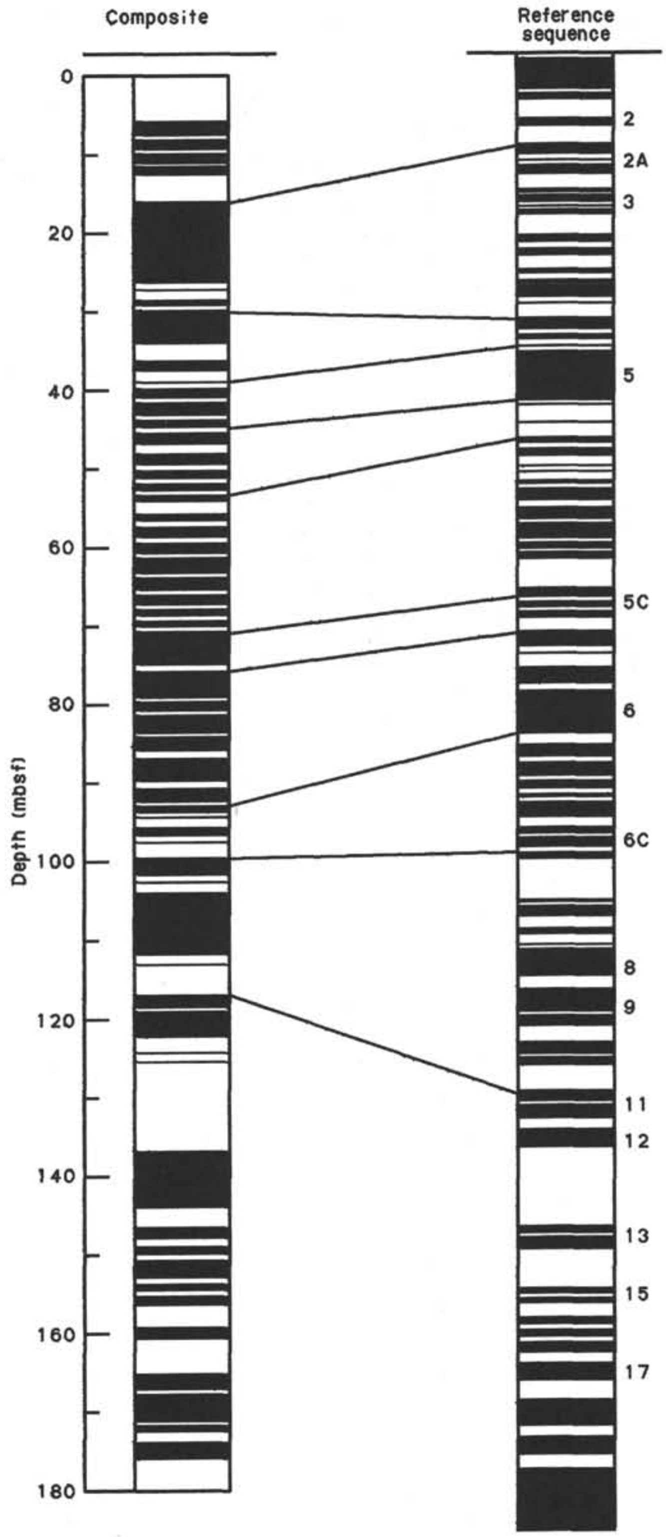

Figure 8. Comparison of the composite magnetic polarity sequence from Holes 744A and 744B to the reference sequence of Berggren et al. (1985). The tie lines between the observed reversal stratigraphy and the reference sequence are based upon the biostratigraphic zonations discussed in the text.

larity zone has been correlated with seafloor anomaly 1 and assigned to the Brunhes Superchron. On the basis of biostratigraphic correlations, a hiatus exists in the sections with the next normal polarity interval correlated with anomaly 2, within the Matuyama Superchron. The oldest polarity event was correlated with a normal polarity interval at 44 Ma, which corresponds to seafloor anomaly 19. Thus, the reversal stratigraphy recorded at Site 744 represents the series of geomagnetic reversals that took place between the late Eocene and Quaternary. Several changes in relative lengths of polarity intervals were observed, indicating that major changes in depositional rates have occurred. A few polarity intervals appear to be absent within this sedimentary sequence, indicating that hiatuses are also present.

SEDIMENTATION RATES

The uppermost Eocene through Pleistocene biogenous oozes recovered at Site 744 were deposited at an average rate of 4.6 m/m.y. The various biostratigraphic events, their age estimates, and the depth intervals in which they were recognized are presented in Table 4. The events are plotted against depth below seafloor in Figure 9. The current resolution is limited to core-catcher samples and will have to be refined by additional shore-based studies of samples within cores. Nevertheless, the following temporal changes seem to be indicated.

The uppermost Eocene through lower Oligocene nannofossil oozes were deposited at a rate of 9.9 m/m.y. The sedimentation rate decreased during the late Oligocene/early Miocene to an average of only 1.6 m/m.y., but increased in the Miocene nannofossil oozes to an average of 5.3 m/m.y. A hiatus of about 5-m.y. duration (or possibly two shorter ones) may represent the latest Miocene to Pliocene time interval (8.4–3.2 Ma). The younger Neogene diatom oozes were deposited at an average rate of 7.0 m/m.y., which is low considering the relatively high porosities of these young sediments.

Table 4. Biostratigraphic events identified at Site 744.

Biostratigraphic event[a]	Depth (mbsf)	Age (Ma)
LAD *Actinocyclus ingens*	0.1-9.5	0.65
LAD *Coscinodiscus kolbei*	9.5-12.0	1.89
LAD *Nitzschia interfrigidaria*	9.5-12.0	2.8
FAD *Theocalyptra davisiana*	13.7-19.0	2.6-2.8
LAD *Prunopyle titan*	19.0-21.5	3.2
FAD *Nitzschia weaveri*	20.8-21.5	3.3-3.4
FAD *Pseudocubus vema*	19.0-21.5	3.9
LAD *Triceraspyris coronata*	19.0-21.5	4.2
FAD *Nitzschia angulata*	21.5-22.2	4.0-4.1
FAD *Desmospyris spongiosa*	21.5-23.2	4.3
LAD *Thalassiosira miocenica*	21.5-22.2	5.1
FAD *Thalassiosira miocenica*	23.4-23.9	6.1
LAD common *Denticulopsis hustedtii*	23.4-23.9	7.1
LAD *Denticulopsis dimorpha*	23.4-23.9	8.4
FAD *Clathrocyclas bicornis spongothorax*	51.7-59.5	9.5-9.8
LAD common *Denticulopsis dimorpha*	34.6-39.1	10.0
LAD *Nitzschia denticuloides*	50.0-53.7	11.0-11.1
LAD *Reticulofenestra hesslandii*	52-61	12
FAD *Denticulopsis praedimorpha*	53.7-58.2	12.8
FAD common *Denticulopsis hustedtii*	53.7-58.2	13.8
FAD *Denticulopsis hyalina*	59.5-67.2	15.0
LAD *Nitzschia maleinterpretaria*	69.0-69.6	15.6
LAD *Globorotalia zealandica*	61.2-70.7	17.6
LAD *Catapsydrax dissimilis*	61.2-70.7	17.6
FAD *Globorotalia praescitula*	80.2-89.7	17.7
FAD *Denticulopsis nicobarica*	74.1-75.6	17.8
FAD *Nitzschia maleinterpretaria*	93.3-97.8	18.8
FAD *Rocella gelida* var. *schraderi*	101.3-107.3	23.6
LAD *Reticulofenestra bisecta*	99-109	25.4
LAD *Chiloguembelina cubensis*	108.7-118.2	30.0
LAD *Globigerina angiporoides*	118.2-127.7	32.0
FAD *Cyclicargolithus abisectus*	118-128	34.2
LAD *Reticulofenestra umbilica*	118-128	34.6
LAD *Isthmolithus recurvus*	137-147	34.9
LAD *Globigerina ampliapertura*	147.6-157.1	32.8
LAD *Globigerinatheka index*	157.1-166.6	36.6
LAD *Reticulofenestra reticulata*	157-167	37.4
FAD *Isthmolithus recurvus*	167-176	37.8

[a] FAD = first-appearance datum; LAD = last-appearance datum.

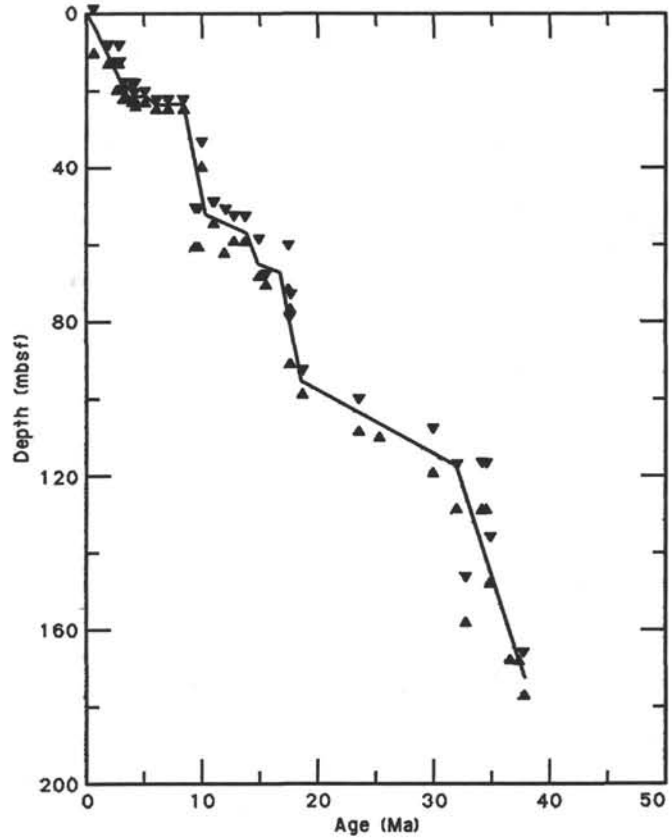

Figure 9. Biostratigraphic events identified at Site 744 (Table 4).

INORGANIC GEOCHEMISTRY

Three holes were cored in 2307.3 m of water at Site 744 on the southern Kerguelen Plateau. Sixteen whole-round minicores, 5 cm in length, were obtained for the purpose of interstitial-water chemical studies. Samples from Holes 744A and 744B were collected in accordance with the routine ODP interstitial-water sampling program (see "Explanatory Notes" chapter). Hole 744C samples were analyzed in cooperation with a 5-yr study to determine the geriatric effects of ODP core storage procedures. Ten samples were taken from the Pliocene to Quaternary diatomaceous and foraminiferal oozes of lithologic Unit I (0–23 mbsf; see "Lithostratigraphy and Sedimentology" section, this chapter). The remaining six samples consist of Eocene to Miocene calcareous ooze from lithologic Unit II. The minicore sediments contain 0.2%–96.2% calcium carbonate. Organic carbon contents of the minicore samples were not available for inclusion in this report.

Results

Site 744 interstitial-water samples were analyzed for pH, alkalinity, salinity, chloride, sulfate, magnesium, calcium, phosphate, ammonium, and silica using the methods outlined in the "Explanatory Notes" chapter. Charge-balance calculations were performed on each of the interstitial-water samples to check for gross irregularities in the data. Sodium and potassium concentrations were calculated by multiplying the ratio of each cation to chloride for average seawater (Stumm and Morgan, 1981) by the chloride concentration of each sample. All of the samples have charge imbalances <2%, indicating that drilling contamination was minimal and that the waters have a seawater origin. Sample 119-744A-3H-3, 145-150 cm, showed obvious signs of drilling disturbance and probably contains some seawater. Results of the sulfate analyses are not available at this time. All of the data obtained at Site 744 are displayed in Table 5.

Salinity and Chloride

A slight increase in interstitial-water chloride concentrations occurs with increasing depth at Site 744 (Fig. 10). Samples in the uppermost 6 mbsf have a mean chloride concentration of 547 mmol/L (s.d. = 1 mmol/L, n = 6); samples between 7 and 163 mbsf have a mean chloride concentration of 557 mmol/L (s.d. = 2 mmol/L, n = 10). The shallowest samples have chloride concentrations that are similar to those of seawater samples collected in this area. Higher chloride concentrations at greater depths may be relic indicators of more saline ocean bottom waters during the last major glacial expansion.

Magnesium and Calcium

Dissolved magnesium and calcium concentrations are well correlated (r = −0.958, n = 16) between the seafloor and 163 mbsf at Site 744 (Figs. 10 and 11). Interstitial-water magnesium concentrations decrease 9%, and calcium concentrations increase 62% with increasing depth between 1 and 163 mbsf. Linear relationships between magnesium and calcium concentrations in interstitial waters have been shown to indicate conservative behavior for these cations (McDuff and Gieskes, 1976; McDuff, 1978; Gieskes, 1983). Thus, the sediments cored at Site 744 are acting as a conduit for the diffusion of magnesium and calcium ions between an oceanic magnesium source and calcium sink and a deep (i.e., deeper than 163 mbsf) sedimentary magnesium sink and calcium source. The linear concentration vs. depth profiles of these cations are indicative of low sediment-accumulation rates and uniform diffusion pathways in the upper 163 mbsf.

Silica

The concentration of silica in the interstitial waters at Site 744 appears to follow the concentration of biogenic silica in the sediments (Fig. 10). Smear slide studies indicate that the abundance of biogenic silica is relatively high in lithologic Unit I (up to 70% diatom frustules; see "Lithostratigraphy and Sedimentology" section) and then sharply decreases below 20 mbsf. Dissolved silica concentrations are relatively high in the uppermost 7 mbsf (mean = 698 μmol/L, s.d. = 26 μmol/L, n = 6) and then decrease 15% immediately below this level. The source of the dissolved silica is the dissolution of biogenic silica in the sediments. The concentration of silica increases with increasing depth in interstitial waters between 47 and 143 mbsf. This increase may be due to a zone of more active silica dissolution and/or greater silica abundance near 140 mbsf. Although most of the sediments at Site 744 contain some biogenic silica, the concentration of silica in the interstitial waters never rises much higher than 50% of its saturation level with respect to biogenic silica (i.e., 1200-1500 μmol/L). The relatively low sediment-accumulation rates at Site 744 allow most of the silica produced below the seafloor to escape to the overlying water column.

pH, Alkalinity, Sulfate, Ammonium, and Phosphate

Analyses for chemical tracers that are sensitive to the catabolism of organic matter in sedimentary systems indicate that little reactable organic matter is being incorporated into the sediments at Site 744 (Fig. 10). The pH, alkalinity, sulfate concentration, and ammonium concentration of interstitial waters between 1 and 163 mbsf are all essentially the same as in seawater. Only the samples above 7 mbsf have phosphate concentrations near or above the detection limit of the analytical procedure (around 2 μmol/L). All of the organic matter deposited on the seafloor at Site 744 apparently is thoroughly oxidized before it can be incorporated into the sediments. These data support the conclusion that sediment-accumulation rates have been relatively low (i.e., <5 m/m.y.) at this site.

ORGANIC GEOCHEMISTRY

Organic geochemistry was studied on squeeze cakes of interstitial-water studies, carbonate, and physical-properties samples (0-176.1 mbsf from Hole 744A, 0-78.5 mbsf from Hole 744B, and 0-26.0 mbsf from Hole 744C), as outlined in the "Explanatory Notes" chapter.

Hydrocarbon Gases

The headspace procedure was used approximately every 30 m to determine hydrocarbon gases. All of the samples had <5 ppm methane. No ethane was detected at Site 744.

Carbon Analysis

Inorganic carbon was measured on all of the interstitial-water squeeze-cake, carbonate, and physical-properties samples (see Table 6 and Fig. 12 for carbonate data).

The 25-mbsf sample interval is characterized by large fluctuations in carbonate from 0% to 65%. Downhole, the carbonate is approximately 90%, varying from 60% to 96% (see "Biostratigraphy" section).

Table 5. Interstitial-water geochemical data for Site 744.

Sample (interval in cm)	Depth (mbsf)	Volume (mL)	pH	Alkalinity (mmol/L)	Salinity (g/kg)	Magnesium (mmol/L)	Calcium (mmol/L)	Chloride (mmol/L)	Phosphate (μmol/L)	Ammonium (mmol/L)	Silica (μmol/L)	Mg^{2+}/Ca^{2+}
744A-1H-2, 145-150	2.95	45	7.6	2.99	35.5	52.5	11.0	548	3	0.00	714	4.8
744A-3H-3, 145-150	18.15	40	7.5	2.51	35.0	52.7	11.0	546	1	0.01	596	4.8
744A-4H-2, 145-150	26.15	40	7.6	2.94	36.0	52.5	11.7	555	1	0.00	605	4.5
744A-6H-3, 145-150	46.65	18	7.5	2.74	35.8	51.6	12.4	556	0	0.01	605	4.2
744A-10H-3, 145-150	84.65	40	7.6	2.87	35.8	50.0	14.2	558	0	0.00	640	3.5
744A-13H-4, 145-150	114.65	35	7.4	2.73	36.2	49.1	15.4	560	0	0.00	656	3.2
744A-16H-4, 145-150	143.15	40	7.3	2.74	36.0	48.7	16.7	558	0	0.00	723	2.9
744A-19H-4, 145-150	163.05	35	7.3	2.79	36.5	47.9	17.3	560	0	0.00	620	2.8
744B-2H-6, 139-144	18.39	60	7.4	2.81	36.2	52.7	11.2	554	1	0.00	667	4.7
744C-1H-1, 145-150	1.45	40	7.5	2.85	35.5	52.7	10.7	548	4	0.00	718	4.9
744C-1H-2, 145-150	2.95	43	7.5	3.03	35.2	52.4	10.9	548	4	0.00	682	4.8
744C-1H-3, 145-150	4.45	50	7.5	3.02	35.5	51.8	11.0	548	2	0.01	672	4.7
744C-1H-4, 145-150	5.95	52	7.5	2.97	35.8	52.5	11.0	546	2	0.00	672	4.8
744C-1H-5, 90-95	6.90	40	7.5	3.00	35.2	53.9	11.3	557	2	0.01	732	4.8
744C-2H-4, 145-150	12.95	35	7.5	2.97	36.0	52.7	11.4	552	1	0.00	614	4.6
744C-3H-4, 145-150	22.45	62	7.4	2.82	36.0	52.7	11.5	556	1	0.00	612	4.6

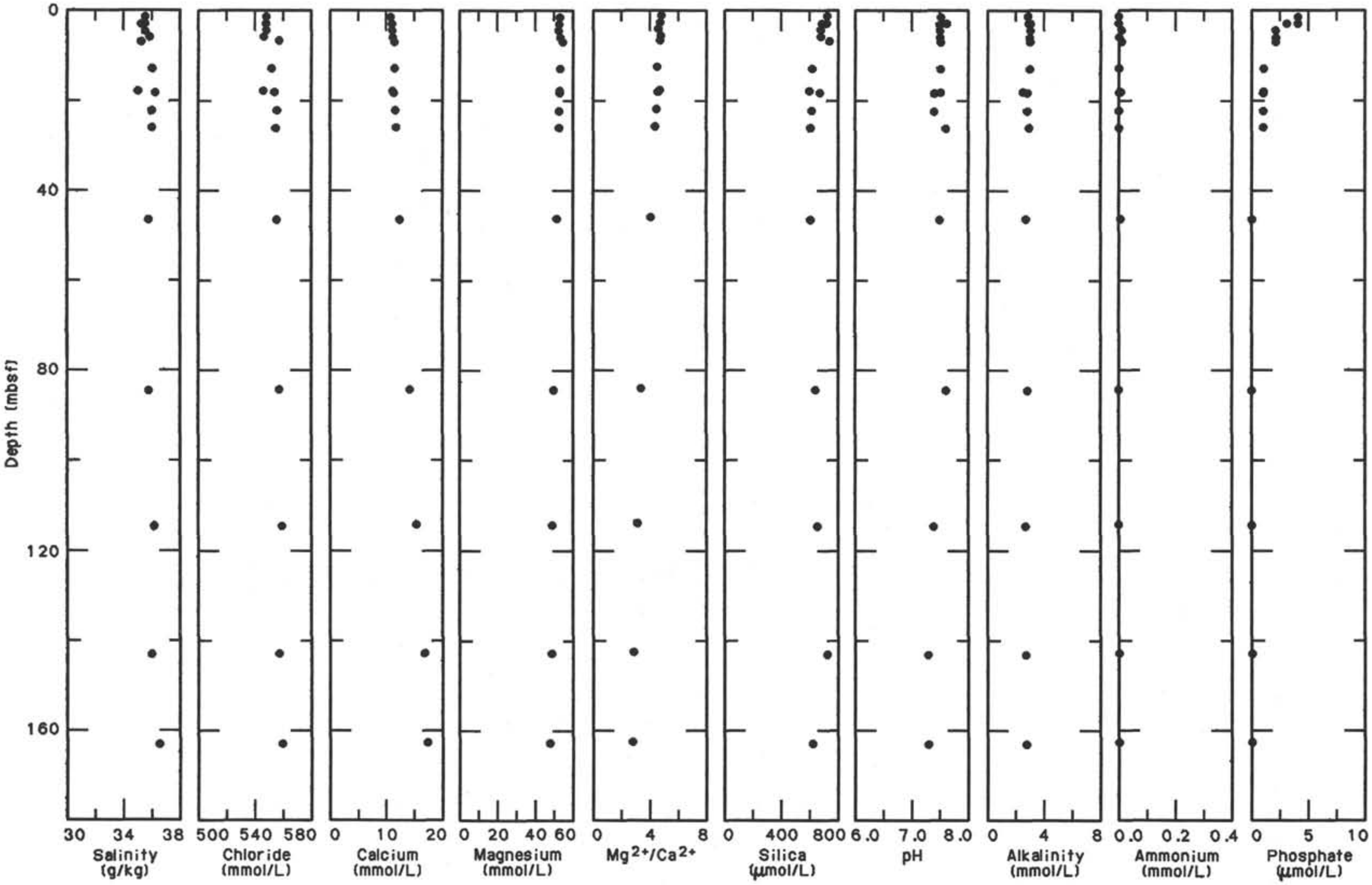

Figure 10. Interstitial-water profiles, Site 744.

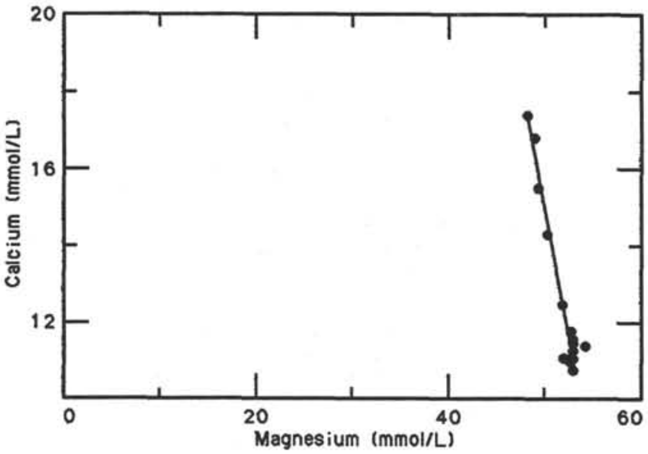

Figure 11. Calcium concentration vs. magnesium concentration plot for Site 744 interstitial waters. The regression line passes through data points representing interstitial-water samples in the upper 163 mbsf and has a slope of −1.21 (r = −0.958).

BIOLOGY AND OCEANOGRAPHY

Physical Characteristics of the Air/Sea Interface

Moderate winds of 10–15 kt from the northwest shifted to southwest during the first 36 hr at Site 744, 5–7 January 1988. On the last day, a light wind remained from the southwest (Table 7). Surface-seawater temperatures of +1.2° to +1.6°C were recorded at the drilling vessel. The water was clearer than at Site 743, although the Secchi disc still disappeared at the relatively shallow depth for open-ocean water of 7 m, indicating a euphotic depth of around 19 m. A hydrocast (61°33.1′E, 80°36.0′S) from the support vessel, *Maersk Master*, registered surface salinity of 34‰. Records transcribed from traces of expendable bathythermographs deployed in the area of the drilling vessel while in transit, before occupation, and after completion of the site are shown in the bathythermograph log (Table 8 and Fig. 13). As the ship traveled north, the cold water inclusion came closer to the surface.

Phytoplankton

Phytoplankton were sampled by using a horizontal (surface) tow and vertical hauls of opening and closing 35-μm mesh nets, as well as by a vertical haul of a 64-μm net from 200 m. Water samples were filtered for later analysis of chlorophyll *a* and estimates of cells per liter. A raw water sample (+0.9°C, 34.0‰ salinity) was refrigerated for culturing in a shorebased study. The three-tiered sediment trap (50, 100, and 200 m) was again deployed and recovered, with analysis of samples to be part of a shorebased study.

The phytoplankton were most similar in species composition to those previously sampled at Site 738. Although they constitute an Antarctic summer assemblage, still dominated by the diatom genera *Rhizosolenia, Chaetoceros*, and *Nitzschia*, some marked differences appear. The collections from all depths looked healthy and were quite similar, except for grazers. *Synedra reinboldii* was more abundant, with clusters of the long, slender cells held together at the base pole. Discoid centric diatoms were not great in number, but they appeared more frequently in the top 50 m than they did at Site 738. Although the southern forms of *Thalassiosira tumida* and *Eucampia antarctica* were present at this site, the northern form of *E. antarctica* was rare, though present. Apparently this is an area of overlapping geographical distribution, although some transient mixing of water masses may occur, perhaps by warm core-ring mesoscale fea-

Table 6. Inorganic and carbonate carbon at Site 744.

Sample (interval in cm)	Depth (mbsf)	Inorganic carbon (%)	$CaCO_3$ (%)
744C-1H-1, 25–26	0.25	2.03	16.9
744C-1H-1, 125–126	1.25	4.76	39.7
744C-1H-2, 25–26	1.75	3.00	25.0
744C-1H-2, 112–113	2.62	4.83	40.2
744A-1H-2, 115–116	2.65	6.89	57.4
744A-1H-2, 145–150	2.95	7.01	58.4
744C-1H-3, 25–26	3.25	6.32	52.7
744A-1H-CC, 0–1	3.93	7.35	61.2
744C-1H-3, 112–113	4.12	6.57	54.7
744C-1H-4, 25–26	4.75	7.70	64.1
744A-2H-1, 120–121	5.40	6.98	58.1
744C-1H-4, 112–113	5.62	7.16	59.6
744C-1H-5, 25–26	6.25	6.46	53.8
744A-2H-2, 110–111	6.80	4.49	37.4
744A-2H-4, 69–71	9.39	4.14	34.5
744B-1H-CC, 0–1	9.60	5.39	44.9
744A-2H-CC, 0–1	9.99	3.06	25.5
744B-2H-115–116	13.65	2.34	19.5
744C-3H-1, 25–26	16.75	3.30	27.5
744C-3H-1, 125–126	17.75	0.07	0.6
744A-3H-3, 145–150	18.15	0.13	1.1
744C-3H-2, 25–26	18.25	0.09	0.8
744B-2H-6, 139–144	18.39	0.02	0.2
744B-2H-CC, 0–1	18.44	0.02	0.2
744C-3H-2, 125–126	19.25	0.10	0.8
744A-3H-4, 146–147	19.66	0.01	0.1
744C-3H-3, 25–26	19.75	0.09	0.8
744C-3H-3, 116–117	20.66	0.18	1.5
744C-3H-4, 25–26	21.25	0.13	1.1
744C-3H-4, 125–126	22.25	0.02	0.2
744C-3H-5, 25–26	22.75	0.02	0.2
744C-3H-5, 125–126	23.75	7.83	65.2
744C-3H-6, 25–26	24.25	8.61	71.7
744A-4H-1, 126–127	24.46	9.27	77.2
744C-3H-6, 125–126	25.25	9.71	80.9
744C-3H-7, 25–26	25.75	10.45	87.1
744A-4H-2, 145–150	26.15	9.59	79.9
744A-4H-3, 123–124	27.43	9.12	76.0
744A-4H-CC, 0–1	28.44	10.69	89.1
744B-4H-6, 67–68	29.67	9.92	82.6
744B-4H-CC, 0–1	31.41	10.95	91.2
744B-5H-3, 90–91	34.90	10.92	91.0
744A-5H-2, 97–98	35.17	9.63	80.2
744A-5H-4, 21–22	37.41	8.14	67.8
744A-5H-CC, 0–1	37.66	8.81	73.4
744B-5H-CC, 0–1	40.94	9.53	79.4
744B-6H-2, 90–91	42.90	10.27	85.6
744A-6H-3, 145–150	46.65	11.55	96.2
744A-6H-CC, 0–1	48.12	7.26	60.5
744B-6H-CC, 0–1	49.45	11.45	95.4
744A-7H-6, 30–31	59.00	11.14	92.8
744A-7H-CC, 0–1	59.27	11.23	93.6
744B-7H-CC, 0–1	59.74	7.29	60.7
744A-8H-4, 110–112	66.80	9.46	78.8
744A-8H-CC, 0–1	66.95	10.16	84.6
744B-8H-7, 30–32	68.80	9.67	80.6
744B-8H-CC, 0–1	69.03	9.62	80.1
744B-9H-2, 85–86	71.35	10.60	88.3
744A-9H-CC, 0–1	71.65	11.12	92.6
744B-9H-CC, 0–1	78.00	11.05	92.1
744A-10H-1, 80–81	81.00	10.53	87.7
744A-10H-3, 145–150	84.65	10.60	88.3
744A-10H-CC, 0–1	89.84	10.78	89.8
744A-11H-1, 85–86	90.55	10.63	88.6
744A-11H-6, 76–76	97.76	10.38	86.5
744A-11H-CC, 0–1	98.31	10.53	87.7
744A-12H-3, 90–92	103.10	10.40	86.6
744A-12H-7, 40–43	108.60	10.99	91.6
744A-12H-CC, 0–1	108.90	10.98	91.5
744A-13H-3, 107–108	112.77	10.79	89.9
744A-13H-4, 145–150	114.65	9.68	80.6
744A-13H-7, 30–32	118.00	10.78	89.8
744A-13H-CC, 0–1	118.11	10.60	88.3
744A-14H-2, 80–82	120.50	10.94	91.1
744A-14H-7, 15–17	127.35	10.45	87.1
744A-14H-CC, 0–1	127.55	10.35	86.2

Table 6 (continued).

Sample (interval in cm)	Depth (mbsf)	Inorganic carbon (%)	$CaCO_3$ (%)
744A-15H-1, 60–62	128.30	10.45	87.1
744A-15H-3, 105–106	131.75	9.00	75.0
744A-15H-CC, 0–1	137.40	8.56	71.3
744A-16H-1, 92–93	138.12	10.45	87.1
744A-16H-4, 145–150	143.15	7.60	63.3
744A-16H-CC, 0–1	146.90	9.52	79.3
744A-17H-CC, 0–1	147.17	10.98	91.5
744A-18H-1, 91–92	148.51	10.76	89.6
744A-18H-CC, 0–1	157.10	11.22	93.5
744A-19H-4, 145–150	163.05	11.26	93.8
744A-19H-5, 134–135	164.44	11.15	92.9
744A-19H-CC, 0–1	165.60	11.29	94.1
744A-20H-4, 97–98	172.07	11.23	93.6
744A-20H-CC, 0–1	176.32	11.41	95.1

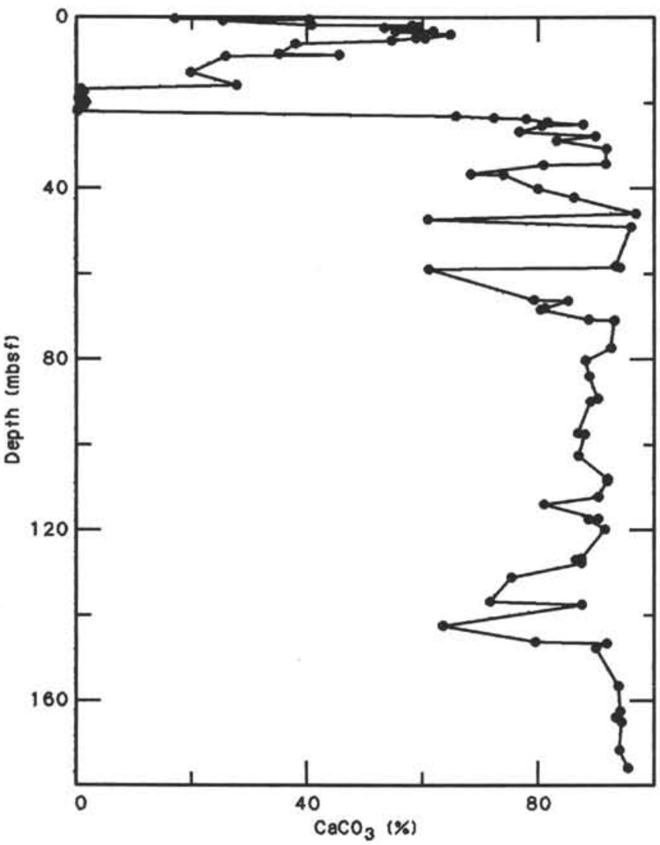

Figure 12. Carbonate carbon at Site 744.

tures. *T. tumida* showed the linear areola pattern (cold-water form; Fryxell, 1988) as well as bundles of areola rows in fascicles. *Nitzschia pseudonana* and *Chaetoceros hendeyi* were present here and not at Site 738. The first is a ubiquitous nannoplanktonic form, poorly collected by nets and easily overlooked, but *C. hendeyi* is vigorous and distinctive.

For the first time the heavily silicified *Thalassiosira trifulta* was seen in chains with cells, joined by threads from the double or triple central processes. The basic strutted process pattern in *Thalassiosira* is of one central process with delicate chain formation, depending on the single thread extruded. Chains of several Antarctic species of *Thalassiosira* are quite distinctive in

Table 7. Wind and weather summary at Site 744 (61.6°5, 80.6°E), February 1988.

5 Feb./1500–2359 hr
Wind: Northwest 12–16 kt.
Sea-surface temperature: 1.2°C.
Waves: 7–8 m.
Sky: Low overcast with light fog and occasional light rain. Pressure falling slightly.
Air temperature: 1.5°C.

6 Feb./0000–2359 hr
Wind: Northwest 10–15 kt shifting to southwest 12–16 kt by 12.00 hr.
Sea-surface temperature: 1.2°–1.5°C.
Waves: 7–8 m.
Sky: Low overcast with occasional fog and drizzle. Pressure slowly rising.
Air temperature: Maximum 2.5°C at 1200 hr
Minimum 0.9°C at 0600 hr.

7 Feb./0000–1500 hr
Wind: Southwest to south 4–8 kt.
Sea-surface temperature: 1.5°–1.6°C.
Waves: 4–5 m.
Sky: Low overcast with occasional light fog and drizzle. Pressure slowly rising.
Air temperature: 1.5°C.

Table 8. Bathythermograph log for Site 744.

Date: 05 Feb 88 Time: 0335Z Location: 62°36′S, 82°47′E		Date: 05 Feb 88 Time: 0930Z Location: 61°53′S, 81°30′E		Date: 07 Feb 88 Time: 1055Z Location: 61°33′S, 80°41′E	
Depth (m)	Temp. (°C)	Depth (m)	Temp. (°C)	Depth (m)	Temp. (°C)
Surface	1.3	Surface	1.2	Surface	1.6
09	1.3	10	1.2	5	2.3
20	0.9	22	2.0	10	2.0
35	0.9	37	1.7	20	0.0
45	−0.2	48	0.0	25	−0.6
62	0.5	55	−0.3	42	0.0
65	1.0	90	0.0	70	1.4
90	1.5	120	1.1	134	2.2
110	1.6	151	2.0	150	2.8
120	1.9	258	2.1	250	2.7
200	2.5	280	2.7	350	3.0
354	2.8	378	3.0		

their possession of thick, almost ropelike twisted threads from multiple central processes. *T. tumida* and *Thalassiosira ritscheri* are other examples of species that make strong chains commonly seen in the water column near Sites 738 and 744.

Few resting spores were seen. *E. antarctica,* although not abundant, was occasionally seen in formation of straight winter stage doublets. *Odontella weissflogii* was present, but only as vegetative cells. Although *Chaetoceros* was abundant, it was mostly from the section Phaeoceros—generally large cells not known to make resting spores.

Grazers were common, especially in the deeper net hauls. Ciliates, copepods, acantharians, and radiolarians were present. Little evidence of krill was apparent. The fecal pellets showed few pigmented cells, but were often full of large diatom frustules, intact but empty.

Diatoms in Surface Sediments

Surface-water sediment and mud-line samples are dominated by *Nitzschia kerguelensis* (Table 9), which forms long chains and is abundant in the plankton at this site. It was present in both coarse and fine forms, and these were seen in the plankton collections and recorded on film, with the outer valves of a chain heavy and coarse and the inner ones with finer structure. The diversity in the sediments is low, with the needlelike *Nitzschia* species, as well as *Chaetoceros,* poorly represented. A few

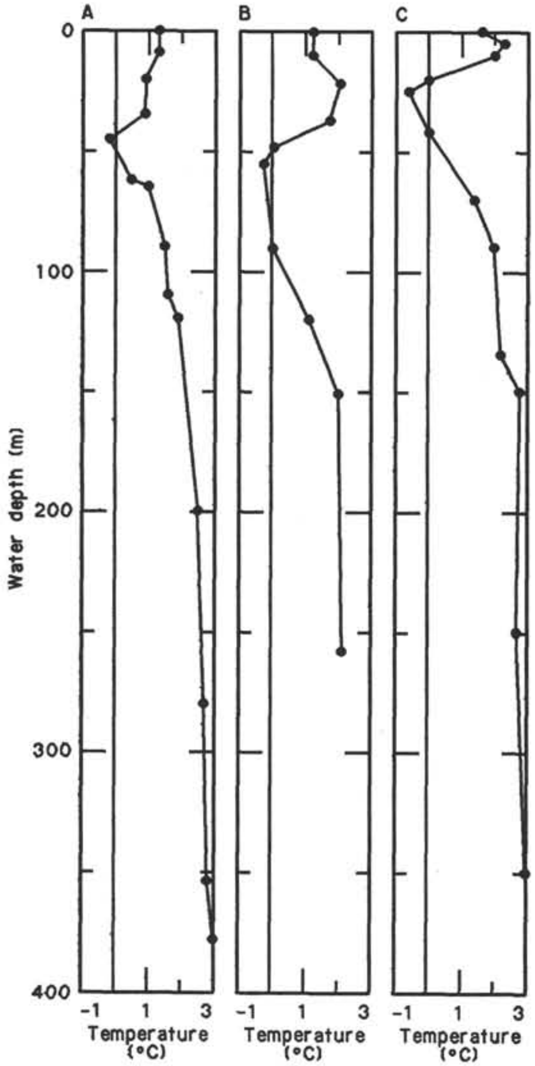

Figure 13. Temperature profiles transcribed from expendable bathythermograph traces. **A.** 5 February 1988, 0335Z; 62°36′S, 82°47′E. **B.** 5 February 1988, 0930Z; 61°53′S, 81°30′E. **C.** 7 February 1988, 1055Z; 61°33′S, 80°41′E.

species indicated that some reworking had occurred or that the mud-line sample was not quite from the surface. Although *Azpeitia tabularis* was confirmed in the sediment, it was not noted from the plankton.

PHYSICAL PROPERTIES

The primary objective of the physical-properties program at Site 744 was to contribute to an understanding of the depositional and post-depositional history of sedimentation on the Kerguelen Plateau. Physical properties measured were (1) index properties (water content, porosity, and bulk density), (2) GRAPE density, (3) undrained shear strength, (4) compressional-wave velocity, and (5) thermal conductivity and temperature. For a discussion of laboratory procedures and techniques, see the "Explanatory Notes" chapter.

Three holes, 744A, 744B, and 744C, were completed at Site 744 by APC to 176.1, 78.5, and 26.0 mbsf, respectively. Core recovery was generally good with minimal coring disturbance.

Physical-properties data are presented in Tables 10 and 11 and Figure 14, except for temperature measurements, which are presented in Table 12 and Figures 15 and 16.

Table 9. Diatoms from the water at the surface of the sediment (Samples 119-744A-1H-1, 0 cm, mud line; 119-744C-1H-1, 0 cm, slurry).

Actinocyclus actinochilus
[a]*A. ingens*
Asteromphalus hyalinus
A. parvulus
Azpeitia tabularis
Coscinodiscus sp.
Dactyliosolen antarcticus (band)
Eucampia antarctica
(straight winter stage doublets, southern form)
[a]*Hemidiscus karstenii*
Nitzschia angulata
N. curta
N. cylindrus
N. kerguelensis
N. obliquecostata
N. ritscherii
N. separanda
Rhizosolenia hebetata f. *semispina*
[a]*Rouxia naviculoides*
[a]*Stictodiscus?* sp.
Thalassiosira gracilis
T. sp. cf. *gravida*
T. lentiginosa
T. oliverana
T. trifulta (band)

[a] Species considered to be extinct.

Results

The sedimentary sequence recovered at Site 744 has been divided into two geotechnical units, G1 and G2, based on the character and trend of physical-properties depth profiles.

Unit G1

Unit G1 (0–25 mbsf) is a diatomaceous ooze with variable carbonate content (see "Organic Geochemistry" section) and significant amounts of clay. Important biogenic components, other than diatoms, are radiolarians and nannofossils. Geotechnical unit G1 correlates roughly with lithologic Unit I (see "Lithostratigraphy and Sedimentology" section).

Average water content (60%), porosity (80%), and bulk density (1.40 g/cm^3) remain fairly constant with depth except for short intervals, which is typical of siliceous oozes. Grain densities are variable and generally high for biogenic silica, probably as a result of the heterogeneous nature of this unit and relatively high abundance of carbonate (high specific gravity). Undrained shear-strength profiles show considerable scatter but exhibit a trend of increasing values with depth. Discrete (Hamilton Frame Velocimeter) velocity measurements show a slightly decreasing trend, while *P*-wave-logger values are nearly constant with depth at 1500 m/s. Thermal conductivity decreases slightly with depth and averages 0.9 W/m/°C.

Unit G2

Unit G2 (25–176 mbsf) is a nannofossil ooze corresponding to lithologic Unit II, which has only relatively small variations in composition (see "Lithostratigraphy and Sedimentology" section). The upper contact is abrupt and distinct on all physical-properties profiles, with the exception of *P*-wave-logger velocities. Velocities of both the Hamilton Frame and *P*-wave logger average 1500 m/s, with only a slight increase to 1550 m/s with depth. Water content and porosity decrease to 45% and 70%, respectively, while bulk and GRAPE densities increase to 1.70 g/cm^3. Shear-strength values decrease sharply to an average of 10 and 30 kPa as determined by vane and fall cone, re-

Table 10. Physical properties measured at Site 744.

Core, section, interval (cm)[a]	Depth (mbsf)	Water content (%)	Porosity (%)	Bulk density (g/cm^3)	Dry-bulk density (g/cm^3)	Gain density (g/cm^3)	Undrained shear strength (kPa)	Compressional-wave velocity[b] (m/s)
119-744A-								
1H-1, 104	1.04						2.6	
1H-1, 105	1.05	67.66	81.63	1.26	0.41	2.12	4.1	
1H-1, 109	1.09							1509.9
1H-2, 115	2.65	51.68	72.56	1.50	0.73	2.49	6.2	1559.2
1H-2, 117	2.67						6.6	
1H-3, 76	3.76						8.5	
1H-3, 78	3.78	49.87	72.45	1.52	0.76	2.67	9.0	
1H-3, 80	3.80							1563.3
2H-1, 120	5.40	56.34	75.15	1.39	0.61	2.36	8.3	
2H-2, 121	5.41						6.4	
2H-1, 123	5.43							1593.5
2H-2, 107	6.77							
2H-2, 110	6.80	73.01	83.32	1.35	0.37	1.82	6.0	1524.2
2H-3, 121	8.41	60.30	79.89	1.44	0.57	2.63		1536.9
2H-3, 122	8.42						9.0	
2H-3, 124	8.44						6.2	
2H-4, 68	9.38						12.4	
2H-4, 69	9.39	62.63	81.02	1.38	0.51	2.56		
2H-4, 70	9.40						21.0	
2H-4, 72	9.42							1496.4
3H-4, 82	19.02							1523.5
3H-4, 83	19.03						11.0	
3H-4, 85	19.05	60.29	78.32	1.36	0.54	2.39		
3H-4, 88	19.08						4.6	
3H-4, 145	19.65						11.2	
3H-4, 146	19.66	56.02	75.84	1.27	0.56	2.48		
3H-4, 147	19.67						18.0	
3H-4, 148	19.68							1529.6
4H-1, 126	24.46	42.32	65.29	1.62	0.93	2.59	12.0	
4H-1, 128	24.48						33.0	
4H-1, 129	24.49							1501.8
4H-2, 92	25.62	46.44	69.91	1.56	0.84	2.71		
4H-2, 93	25.63						11.4	
4H-2, 94	25.64						24.0	
4H-2, 95	25.65							1484.0
4H-3, 122	27.42						25.0	1490.9
4H-3, 123	27.43	44.48	68.16	1.61	0.90	2.70		
4H-3, 125	27.45						10.8	
5H-2, 96	35.16						12.0	
5H-2, 97	35.17	42.35	66.13	1.67	0.96	2.69		
5H-2, 98	35.18						30.0	
5H-2, 99	35.19							1484.4
5H-3, 74	36.44	47.36	69.66	1.54	0.81	2.58	16.3	
5H-3, 76	36.46						38.0	
5H-3, 77	36.47							1483.7
5H-4, 20	37.40						28.0	1492.5
5H-4, 21	37.41	47.04	68.21	1.53	0.81	2.44		
5H-4, 23	37.43						11.6	
6H-1, 85	43.05	37.64	62.67	1.75	1.09	2.82	17.0	1576.9
6H-2, 85	44.55						4.6	
6H-4, 77	47.47	37.67	63.30	1.81	1.13	2.89	1.9	1544.0
7H-1, 125	52.95	43.51	67.33	1.72	0.97	2.71	35.0	
7H-2, 127	54.47	36.96	63.12	1.84	1.16	2.96	23.2	1556.1
7H-4, 105	57.25							1544.0
7H-6, 30	59.00	36.67	61.41	1.79	1.14	2.78	24.2	1527.8
8H-1, 80	62.00	44.97	70.31	1.66	0.92	2.93	21.9	1515.0
8H-2, 110	63.80						22.8	
8H-2, 115	63.85	40.09	65.52	1.76	1.05	2.88	27.0	1538.1
8H-4, 110	66.80	40.18	65.71	1.81	1.09	2.89	17.8	1568.3
9H-1, 70	71.40	37.21	63.50	1.42	0.89	2.97	7.4	1523.6
10H-1, 80	81.00	42.50	66.80	1.68	0.90	2.76	13.9	1566.5
10H-3, 66	83.86	39.40	65.70	1.75	1.00	2.98	4.3	1522.6
10H-4, 88	85.58	40.40	61.70	1.64	0.90	2.40	8.3	
10H-6, 87	88.57						3.7	
10H-7, 45	89.65						27.0	1545.1
11H-1, 85	90.55	36.70	59.30	1.77	1.12	2.55	12.0	1526.0
11H-3, 110	93.80	36.40	57.60	1.75	1.10	2.40	10.6	1545.0
11H-5, 110	96.80	37.60	61.50	1.80	1.12	2.68	14.9	1543.1
11H-6, 76	97.96	39.10	62.70	1.75	1.00	2.65	17.4	1555.1
12H-1, 85	100.05						25.9	1549.6
12H-3, 90	103.10						7.9	1541.0
12H-4, 91	104.61						9.7	1586.2
12H-5, 130	106.50						20.7	1523.8
12H-7, 40	108.60	33.39	57.22	1.82	1.21	2.70	9.9	

Table 10 (continued).

Core, section, interval (cm)[a]	Depth (mbsf)	Water content (%)	Porosity (%)	Bulk density (g/cm³)	Dry-bulk density (g/cm³)	Gain density (g/cm³)	Undrained shear strength (kPa)	Compressional-wave velocity[b] (m/s)
13H-1, 94	109.64	35.44	60.93	1.83	1.18	2.88	8.9	1529.9
13H-3, 107	112.77	38.22	62.28	1.82	1.12	2.70	8.1	1548.9
13H-5, 70	115.40	35.32	61.56	1.88	1.22	2.97	11.8	1517.1
13H-7, 30	118.00	35.73	60.13	1.78	1.14	2.75	9.7	1538.8
14H-2, 80	120.50						10.3	1559.0
14H-4, 78	123.48	35.66	59.50	1.85	1.19	2.69	8.5	1587.4
14H-6, 132	127.02	37.78	62.55	1.80	1.12	2.79	14.5	1583.0
14H-7, 15	127.35	38.83	62.39	1.87	1.15	2.65	13.7	1570.2
15H-1, 60	128.30	37.61	61.45	1.77	1.11	2.68	23.6	1528.9
15H-3, 105	131.75	42.92	66.15	1.68	0.96	2.63	26.9	1493.9
15H-5, 97	134.67	39.59	66.75	1.81	1.09	3.10	11.6	1552.6
16H-1, 92	138.12	38.33	61.19	1.69	1.04	2.57	11.4	1567.8
16H-3, 120	141.40	44.91	67.50	1.62	0.90	2.57	9.9	1548.2
16H-5, 87	144.07	40.53	66.52	1.78	1.06	2.95	6.2	1547.2
16H-7, 20	146.40	45.00	71.01	1.66	0.91	3.03	14.3	1564.1
17H-1, 40	147.10	42.21	65.95	1.74	1.00	2.68		1547.5
18H-1, 90	148.50						11.2	
18H-1, 91	148.51	40.32	65.16	1.68	1.00	2.80	23.0	
18H-1, 92	148.52							1493.9
18H-2, 103	150.13						4.3	
18H-2, 105	150.15						17.0	
18H-2, 107	150.17							1488.6
18H-3, 103	151.63						6.0	
18H-3, 107	151.67							1518.8
18H-3, 108	151.68						17.0	
18H-5, 66	154.26						14.0	
18H-5, 68	154.28						6.0	
18H-5, 69	154.29	37.76	62.07	1.74	1.08	2.73		
18H-5, 71	154.31							1506.0
19H-1, 67	157.77						21.7	
19H-1, 69	157.79	35.24	60.36	1.82	1.18	2.83		
19H-1, 71	157.81						56.0	
19H-3, 62	160.72							1513.0
19H-3, 63	160.73	36.21	60.77	1.80	1.15	2.76	54.0	
19H-3, 66	160.76						26.9	
19H-5, 130	164.40						54.0	
19H-5, 132	164.42						27.3	
19H-5, 134	164.44	34.98	58.51	1.76	1.14	2.66		
19H-5, 135	164.45							1524.9
19H-CC, 19	165.79	34.08	58.22	1.79	1.18	2.73		
19H-CC, 21	165.81						27.5	
19H-CC, 23	165.83							1470.3
20H-2, 109	169.19						10.6	
20H-2, 110	169.20	35.79	60.70	1.82	1.17	2.81		
20H-2, 113	169.23						36.0	1517.3
20H-4, 96	172.06						12.6	
20H-4, 97	172.07	33.70	59.91	1.85	1.22	2.98		
20H-4, 99	172.09						51.0	
20H-4, 100	172.10							1512.0
20H-6, 100	175.10						20.3	
20H-6, 101	175.11	32.51	58.38	1.89	1.28	2.95		
20H-6, 102	175.12						48.0	
20H-6, 103	175.13							1544.0
20H-7, 20	175.80							1542.4
20H-7, 21	175.81						42.0	
20H-7, 23	175.83						13.9	
20H-7, 25	175.85	34.15	58.13	1.84	1.21	2.71		
119-744B-								
1H-1, 108	1.08	60.91	79.20	1.36	0.53	2.45		
1H-1, 111	1.11						18.0	
1H-1, 112	1.12							1586.1
1H-3, 96	3.96							1533.9
1H-3, 97	3.97	48.83	71.17	1.52	0.78	2.61	27.0	
1H-3, 100	4.00						9.3	
1H-5, 65	6.65	55.84	77.43	1.45	0.64	2.73	11.8	
1H-5, 67	6.67						28.0	
1H-5, 68	6.68							1544.3
1H-7, 20	9.20						20.0	
1H-7, 22	9.22						13.7	
1H-7, 23	9.23	66.81	84.28	1.35	0.45	2.67		
1H-7, 24	9.24							1536.8
2H-1, 95	10.45							1501.1
2H-1, 98	10.48	63.81	79.73	1.33	0.48	2.23	16.0	
2H-1, 100	10.50						9.3	

Table 10 (continued).

Core, section, interval (cm)[a]	Depth (mbsf)	Water content (%)	Porosity (%)	Bulk density (g/cm³)	Dry-bulk density (g/cm³)	Gain density (g/cm³)	Undrained shear strength (kPa)	Compressional-wave velocity[b] (m/s)
2H-3, 114	13.64						7.7	
2H-3, 116	13.66						8.4	
2H-3, 117	13.67							1487.4
2H-4, 70	14.70							1534.7
2H-5, 66	16.16						29.0	
2H-5, 68	16.18	63.96	79.37	1.32	0.47	2.17		
2H-5, 70	16.20						39.9	
4H-2, 70	23.70						12.2	
4H-2, 73	23.73	45.81	69.06	1.60	0.87	2.67	25.0	1491.2
4H-4, 142	27.42							1470.3
4H-4, 143	27.43	43.82	66.85	1.61	0.90	2.61		
4H-4, 145	27.45						14.7	
4H-6, 66	29.66						9.7	
4H-6, 67	29.67	43.61	67.74	1.63	0.92	2.75		
4H-6, 69	29.69						25.0	
4H-6, 70	29.70							1451.3
4H-7, 61	31.11	42.48	66.02	1.68	0.97	2.66		1487.9
4H-7, 62	31.12						30.0	
4H-7, 64	31.14						11.6	
5H-3, 90	34.90	42.55	69.13	1.76	1.01	3.06	10.3	1524.5
5H-6, 92	39.42	46.03	66.26	1.57	0.84	2.32	16.5	1508.7
6H-2, 95	42.95	42.66	64.44	1.60	0.92	2.46	7.2	1507.4
6H-4, 113	46.13	38.11	63.70	1.79	1.11	2.89	1.7	1521.5
6H-6, 94	48.94	38.60	65.01	1.75	1.08	2.99	1.0	1533.7
7H-2, 100	52.50	35.43	60.87	1.81	1.17	2.87	6.8	1545.5
7H-4, 98	55.48	36.85	62.32	1.78	1.12	2.87	15.9	1540.7
7H-7, 30	59.30	62.49	79.75	1.35	0.51	2.37	12.6	1535.2
8H-2, 93	61.93						24.4	
8H-2, 102	62.02	37.67	60.75	1.69	1.05	2.59	9.1	1519.4
8H-4, 93	64.93	53.83	72.42	1.49	0.69	2.27	39.0	1515.7
8H-7, 30	68.80	40.73	63.30	1.74	1.03	2.54	2.3	1533.0
9H-2, 85	71.35	38.93	64.28	1.74	1.06	2.86	7.0	
9H-4, 103	74.53	38.21	62.48	1.79	1.11	2.73	4.1	
9H-6, 90	77.40	40.40	64.91	1.93	1.15	2.76	2.7	
119-744C-								
1H-1, 60	0.60	65.70	81.74	1.32	0.45	2.34	1.4	1536.9
1H-1, 110	1.10	70.69	85.62	1.29	0.38	2.46	3.7	1544.0
1H-2, 50	2.00						9.1	1560.0
1H-2, 115	2.65	58.56	79.10	1.43	0.59	2.70	6.6	1599.0
1H-3, 20	3.20	67.58	83.08	1.30	0.42	2.35	8.7	1578.7
1H-3, 70	3.70						30.0	
1H-3, 80	3.80	50.91	72.91	1.51	0.74	2.62	11.4	1580.8
1H-4, 46	4.96	49.19	72.92	1.57	0.80	2.81	6.6	1595.9
1H-4, 90	5.40	54.95	74.42	1.45	0.66	2.40	9.5	1584.2
1H-5, 35	6.35	54.07	77.60	1.53	0.70	2.97	11.0	1603.0
2H-1, 55	7.55	65.48	82.03	1.35	0.46	2.41	9.7	1542.6
2H-1, 115	8.15	64.67	82.23	1.39	0.49	2.53	7.7	1556.2
2H-2, 65	9.15	58.68	78.52	1.52	0.63	2.59	9.9	1561.6
2H-2, 120	9.70	53.98	76.47	1.50	0.69	2.80	6.4	1550.5
2H-3, 30	10.30	62.88	80.13	1.37	0.51	2.39	9.1	1553.9
2H-3, 90	10.90	63.16	81.17	1.38	0.51	2.52	10.6	
2H-4, 40	11.90	60.43	77.89	1.42	0.56	2.31	6.4	1536.7
2H-4, 90	12.40						16.8	1529.1
2H-5, 20	13.20	56.86	79.92	1.58	0.68	3.05	11.2	1645.3
2H-5, 80	13.80	58.07	80.09	1.56	0.65	2.93	7.7	1536.7
2H-6, 29	14.79						18.6	1591.7
2H-6, 100	15.50	57.50	78.09	1.46	0.62	2.65	25.2	1553.5
2H-7, 20	16.20	62.62	84.27	1.48	0.55	3.22	36.4	1596.0
3H-1, 84	17.34						19.7	
3H-1, 87	17.37						24.0	
3H-1, 88	17.38	58.92	77.42	1.37	0.56	2.40		1494.0
3H-1, 135	17.85						22.6	
3H-1, 136	17.86	57.00	75.07	1.37	0.59	2.28		
3H-1, 137	17.87							1539.1
3H-1, 138	17.88						28.0	
3H-2, 16	18.16							1512.6
3H-2, 17	18.17	55.91	74.77	1.38	0.61	2.35		
3H-2, 18	18.18						31.0	
3H-2, 20	18.20						26.2	
3H-2, 106	19.06						24.8	
3H-2, 108	19.08	54.65	70.86	1.31	0.59	2.03	36.0	
3H-2, 113	19.13							1530.4
3H-3, 44	19.94						36.0	1593.5
3H-3, 47	19.97						25.7	

Table 10 (continued).

Core, section, interval (cm)[a]	Depth (mbsf)	Water content (%)	Porosity (%)	Bulk density (g/cm^3)	Dry-bulk density (g/cm^3)	Gain density (g/cm^3)	Undrained shear strength (kPa)	Compressional-wave velocity[b] (m/s)
3H-3, 51	20.01							1508.9
3H-3, 103	20.53						38.0	
3H-3, 104	20.54	62.07	79.72	1.32	0.50	2.41		
3H-3, 106	20.56						28.4	
3H-3, 110	20.60							1516.1
3H-4, 14	21.14						28.9	
3H-4, 15	21.15	62.97	79.53	1.36	0.50	2.29		
3H-4, 16	21.16							1502.1
3H-4, 17	21.17						38.0	
3H-4, 108	22.08						38.1	
3H-4, 109	22.09	58.24	75.20	1.38	0.58	2.18		
3H-4, 110	22.10						39.0	
3H-4, 113	22.13							1557.1
3H-5, 28	22.78							1520.3
3H-5, 38	22.88	59.07	77.63	1.40	0.57	2.42	17.0	
3H-5, 41	22.91						53.0	
3H-5, 108	23.58							1476.3
3H-5, 110	23.60	43.09	67.48	1.64	0.94	2.77	54.0	
3H-6, 14	24.14						23.9	
3H-6, 16	24.16	41.24	66.96	1.74	1.02	2.92	54.0	
3H-6, 17	24.17							1490.5
3H-6, 113	25.13	41.36	64.71	1.66	0.97	2.63	54.0	1520.2
3H-6, 115	25.15						30.7	
3H-7, 9	25.59						29.9	
3H-7, 10	25.60	35.56	60.47	1.74	1.12	2.81		
3H-7, 12	25.62							1501.1
3H-7, 55	26.05						13.3	
3H-7, 58	26.08	39.13	62.83	1.75	1.07	2.66		
3H-7, 59	26.09						51.0	1523.6

[a] Top of interval, never exceeding 10 cm.
[b] Measured with Hamilton Frame.

spectively. Thermal conductivity also increases abruptly to 1.2 W/m/°C at the contact and subsequently increases slightly with depth.

Temperature and Heat Flow

Thermal-conductivity values were measured solely on APC cores. Valid values range from 0.6 to 1.7 W/m/°C and average about 1.2 W/m/°C. Values below 0.59 W/m/°C, the conductivity of water at ambient conditions (Clark, 1966), are considered erroneous.

Temperatures were measured at two sub-bottom depths (80 and 176.1 mbsf) in Holes 744B and 744A, respectively, using the Uyeda probe and standard operational procedures (see "Explanatory Notes" chapter). The temperature measurements were affected somewhat by ship surge of 1–2 m, causing likely vertical motion of the probe while in the sediment. The apparent surge effects (e.g., small peaks on the temperature curve) increase with depth, probably reflecting the greater temperature loss in more indurated rocks caused by gradual probe extraction.

The temperature profile for 80 mbsf in Hole 744B gave a good equilibrium temperature of 5.7°C. Only minor temperature variations appeared during the 20 min that the probe was in the sediment. After this time, a small increase in temperature occurred, followed by pull out.

The temperature at 176.1 mbsf shows three small triangular peaks during penetration. Two attempts at estimating the equilibrium temperature were made. The first estimate was based on the period immediately following initial penetration, and the second estimate was based on a later period, directly following the first (i.e., assumes instantaneous resetting of the probe). The range in estimated equilibrium temperatures (7.7°–9.5°C) gives the likely temperature measurement error.

Temperatures at Site 744 range from about 1.0°C at the seafloor to about 8.5°C at 176.1 mbsf, giving an average temperature gradient of about 43°C/km. The average temperature gradient is not tightly constrained by the three measurements and could vary significantly. The sedimentary section over this interval is composed of nannofossil oozes with conductivity values about 1.2 W/m/°C. The heat flow, based on these averages values for temperature gradient and thermal conductivity, is 51.1 W/m^2 (1.22 HFU).

Summary

Although the depth trends of index properties are nearly constant with depth, small-scale variations occur that are consistent for data from all three holes. The slight decreases in water content and porosity and increases in density appear to be correlated with variations in silica abundance (see "Lithostratigraphy and Sedimentology" section). Below 6 mbsf appears a trend of rapidly decreasing carbonate content (see "Organic Geochemistry" section). This is accompanied by only slight changes in index-property profiles, indicating the importance of biogenic silica, rather than carbonate, in determining the overall trend of the profiles.

While index-property profiles remain relatively constant with depth in the diatomaceous ooze, other properties do show depth-related trends. These trends, however, appear to be anomalous. Velocities in geotechnical unit G1 show a slight decrease with depth. This may be related to either or both trends of decreasing carbonate and increasing biogenic silica within the unit. Thermal conductivity is normally inversely correlated with water content and would be expected to show no significant change with depth in unit G1. Instead, an apparent decrease in conductivity occurs with depth, associated with decreasing carbonate and increasing silica. Undrained shear-strength profiles exhibit normal trends of overall increase with depth. This is anomalous, however, in that shear strength is normally a function of water content and would be expected to show no significant change with depth in unit G1.

Table 11. Thermal conductivity and temperature drift rate for Holes 744A and 744C.

Core, section, interval (cm)	Depth (mbsf)	Thermal conductivity (W/m/°C)	Temperature drift rate (°C/min)
119-744A-			
1H-1, 60	0.60	0.490	0.016
1H-2, 60	2.10	0.932	0.002
1H-3, 60	3.60	1.044	0.051
2H-1, 70	4.90	1.145	0.003
2H-2, 70	6.40	0.794	0.002
2H-3, 70	7.90	0.940	0.002
3H-3, 70	17.40	0.218	0.001
3H-4, 70	18.90	0.872	0.002
5H-1, 70	33.40	0.571	−0.060
5H-2, 70	34.90	1.165	0.044
5H-3, 70	36.40	0.934	0.037
5H-4, 30	37.50	1.247	0.055
6H-1, 70	42.90	1.429	0.092
6H-2, 70	44.40	1.227	0.034
6H-3, 70	45.90	1.269	0.040
6H-4, 70	47.40	1.289	0.030
7H-1, 80	52.50	1.196	0.091
7H-3, 80	55.50	1.246	0.036
7H-5, 80	58.50	1.325	0.056
7H-6, 40	59.10	1.405	0.044
8H-1, 70	61.90	1.166	0.086
8H-2, 70	63.40	1.243	0.046
8H-3, 70	64.90	1.317	0.057
8H-4, 70	66.40	1.199	0.056
9H-1, 50	71.20	0.985	0.055
10H-1, 80	81.00	1.014	0.076
10H-3, 80	84.00	1.278	0.050
10H-5, 80	87.00	1.378	0.062
10H-7, 40	89.60	1.326	0.048
11H-2, 50	91.70	1.319	0.052
11H-4, 50	94.70	1.343	0.029
11H-6, 50	97.70	1.032	0.020
12H-1, 50	99.70	1.238	0.076
12H-3, 50	102.70	1.445	0.044
12H-5, 50	105.70	1.211	0.044
12H-7, 50	108.70	1.403	0.041
13H-1, 70	109.40	1.197	0.177
13H-3, 70	112.40	1.392	0.037
13H-5, 70	115.40	1.546	0.064
13H-7, 35	118.05	1.409	0.049
14H-1, 70	118.90	1.486	0.093
14H-3, 70	121.90	1.329	0.030
14H-5, 0	124.90	1.499	0.047
14H-6, 70	126.40	1.421	0.028
15H-1, 70	128.40	0.893	0.137
15H-4, 70	132.90	1.179	0.026
15H-6, 70	135.90	1.309	0.055
16H-1, 70	137.90	1.006	0.022
16H-3, 70	140.90	1.042	−0.009
16H-5, 70	143.90	1.034	−0.008
18H-2, 70	149.80	1.517	0.053
18H-4, 70	152.80	1.586	0.031
18H-6, 70	155.80	1.734	0.045
19H-2, 70	159.30	1.321	0.091
19H-4, 70	162.30	1.416	0.037
19H-5, 70	163.80	1.478	0.044
19H-6, 70	165.30	1.428	0.042
20H-1, 70	167.30	1.179	0.080
20H-2, 70	168.80	1.257	0.002
20H-4, 70	171.80	1.308	0.052
20H-6, 70	174.80	1.394	0.034
119-744C-			
1H-1, 70	0.70	0.547	0.019
1H-2, 70	2.20	0.940	0.009
1H-3, 70	3.70	1.035	0.001
1H-4, 70	5.20	1.039	0.002
2H-1, 70	7.70	0.736	0.050
2H-2, 70	9.20	0.921	0.002
2H-3, 70	10.70	0.984	0.015
2H-4, 70	12.20	0.896	0.028
2H-5, 70	13.70	0.844	0.030
2H-6, 70	15.20	0.776	−0.026
3H-1, 70	17.20	2.251	0.153
3H-2, 70	18.70	0.627	−0.275
3H-3, 70	20.20	0.837	0.035
3H-4, 70	21.70	0.832	0.017
3H-5, 70	23.20	1.242	0.036
3H-6, 70	24.70	1.288	0.026
3H-7, 45	25.95	0.792	−0.160

Table 12. Temperature measurements for Site 744.

Core	Depth (mbsf)	Time (min) IB	ET	ML	Temperature (°C) T_{SF}	T_M	T_B
119-744B-9H	80.0	23	20	8	0.9	1.3	5.3
119-744A-20H	176.1	28	8	5	1	1.4	8.1

Note: IB = probe in sediment; ET = probe equilibration time; ML = probe at mud line (actually 10 mbsf); T_{SF} = coldest temperature immediately prior to probe penetration; T_M = temperature at 10 mbsf; T_B = equilibration temperature in sediment.

Physical-properties profiles within geotechnical unit G2 exhibit normal, although slight, depth trends in response to overburden. Water content and porosity decrease slightly with depth, while densities and thermal conductivity increase slightly. Shear-strength profiles may be an exception to the characterization of otherwise normal depth-related trends. Fall cone data suggest only a slight increase with depth, while no trend is evident from vane measurements. Fall cone data, while well correlated with vane shear, consistently show higher values. This has been noted by previous authors (Keller and Bennett, 1971) and at other sites on Leg 119 (see "Physical Properties" section, "Site 738" chapter). Fall cone data for unit G2 also show considerable scatter. This variation is real since high and low values are correlative for the two methods used and are duplicated in different holes. Higher values also appear to be roughly correlated with increases in GRAPE density and possibly with increases in diatom content (see "Lithostratigraphy and Sedimentology" section).

SEISMIC STRATIGRAPHY

A single-channel seismic-reflection line was measured by *JOIDES Resolution* as a tieline from the multichannel seismic line MD 47-07, shotpoint 608 (M. Munschy and R. Schlich, pers. comm., 1987), at the target Site SKP-6B to Site 744 (see Fig. 1, "Site Geophysics" section, this chapter). Inspection of the single-channel line suggests a division in four seismic units.

The upper seismic Unit I from the seafloor down to around 3.3 s two-way traveltime (TWT; about 200 mbsf) is characterized by a band of fairly strong, continuous reflections, some of which may be bubble pulse from the water gun. It rests on seismic Unit II (3.3–3.75 s TWT) with very low reflectivity in the top and increasing reflectivity downward. The reflectors are almost horizontal, so the draping pattern seen at Site 738 does not appear. Seismic Unit III is characterized by bands of strong continuous reflectors below 3.75 s TWT, which possibly onlap onto a moderately uneven acoustic basement seismic Unit IV at 3.9 s TWT at the site. The regular reflection pattern indicates a stable deposition pattern through time in this part of the southern Kerguelen Ridge. This is in agreement with the observations of the cored interval.

The boundary between seismic Units I and II is at approximately 200 mbsf at Site 744, assuming a mean sound velocity of 1550 m/s (see "Physical Properties" section, this chapter). Hole 744A was terminated at 176.1 mbsf, so only seismic Unit I was sampled. The boundary probably marks the transition from calcareous nannofossil ooze to chalk, because this diagenetic transition was found at almost the same depth below seafloor and in sediments of similar age and composition at Site 738 about 185 km away. In addition, the first occurrence of micrite overgrowths of coccoliths was observed in the lower cores of Site 744. Thus seismic Unit I at Site 744 consists of 21.3 m of generally calcareous diatom ooze of latest Miocene to Quaternary age and a layer of nannofossil ooze of late Eocene (or slightly older) to late Miocene age. No major hiatus is recognized in the sequence indicated by seismic stratigraphy.

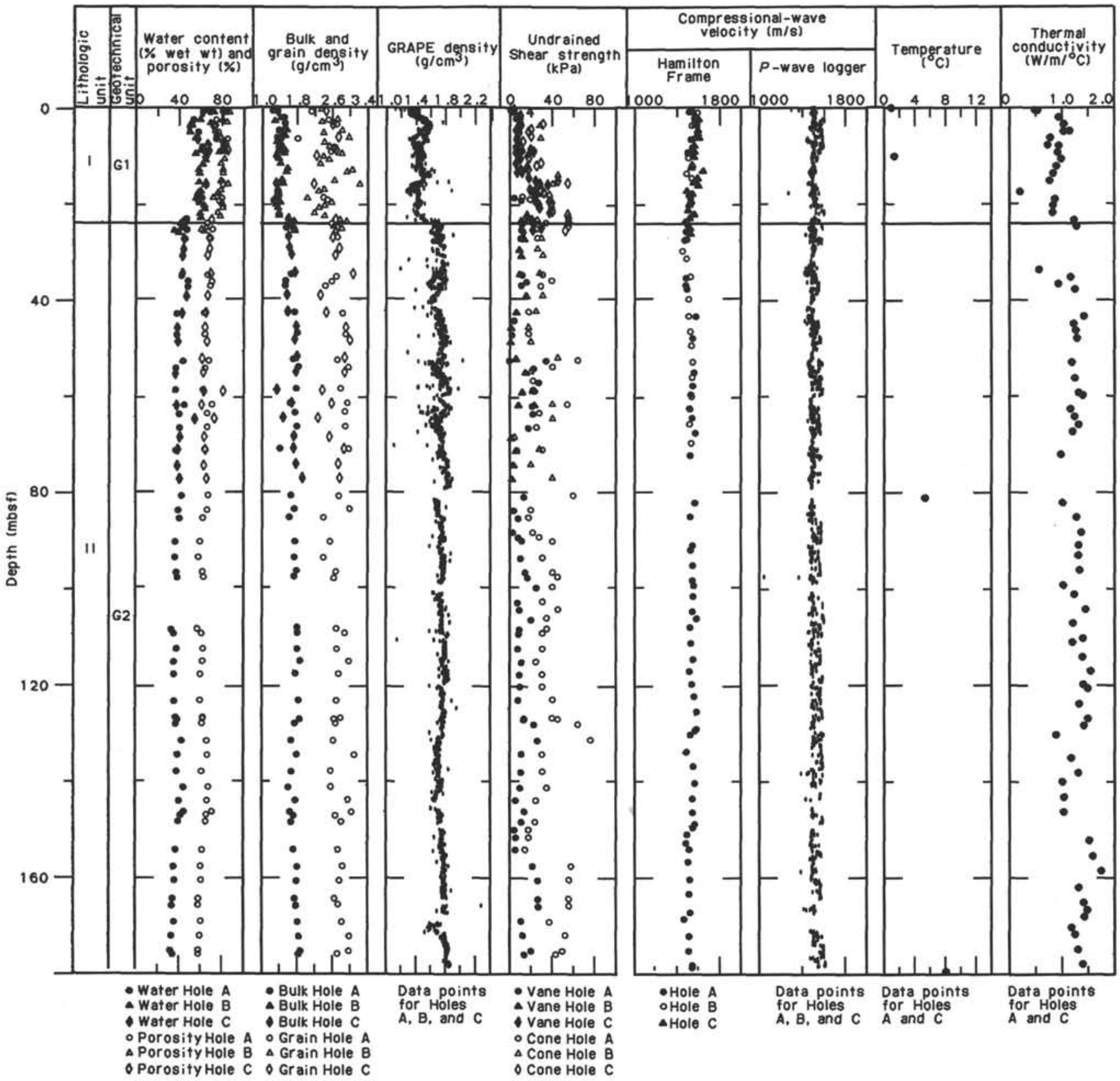

Figure 14. Physical-properties profiles for Site 744.

A seismic stratigraphy was proposed based on the information near Site 738 (see "Seismic Stratigraphy" section, "Site 738" chapter). Seismic Unit I at Site 738 consists of uppermost Miocene to Quaternary diatom ooze with glacial dropstones and may include a thin layer of diatomaceous nannofossil ooze of late Miocene age. This layer rests at Site 738 on lower Oligocene nannofossil ooze, indicating a major hiatus (see "Biostratigraphy" section, "Site 738" chapter). Based on correlation with lithostratigraphy and stratigraphic age, seismic Unit I at Site 744 seems analogous to both seismic Units I and II, as defined at Site 738. However, the base of seismic Unit I at both sites is characterized by a transition from a reflection band to an almost reflection-free unit. Thus, the correlation between the upper seismic units with the lithology and age of the sequences at Site 744 differs significantly from that at Site 738. These observations indicate that seismic Unit I, as an indicator of diatom ooze sediments at Site 738, seems to be too thin for a reliable tracing on the available seismic records and that the seismic expression of the soft nannofossil ooze changes significantly through the area, with the seismic methods used. We therefore concluded that, at present, no useful seismic stratigraphy can be established for the upper unlithified layers of late Eocene to Quaternary age at the southern Kerguelen Plateau.

SUMMARY AND CONCLUSIONS

Site 744 provides an excellent biostratigraphic and magnetostratigraphic reference section for the Oligocene and Neogene of the southern Kerguelen Plateau that complements the excellent Upper Cretaceous to Eocene section obtained at Site 738. A 176.1-m-thick uppermost Eocene to Quaternary section, which contains carbonate throughout, was cored with a composite recovery of 90% in three holes at Site 744. The uppermost Miocene to Quaternary in the upper 23 m of the section is predominantly diatomaceous ooze, with a variable content of carbon-

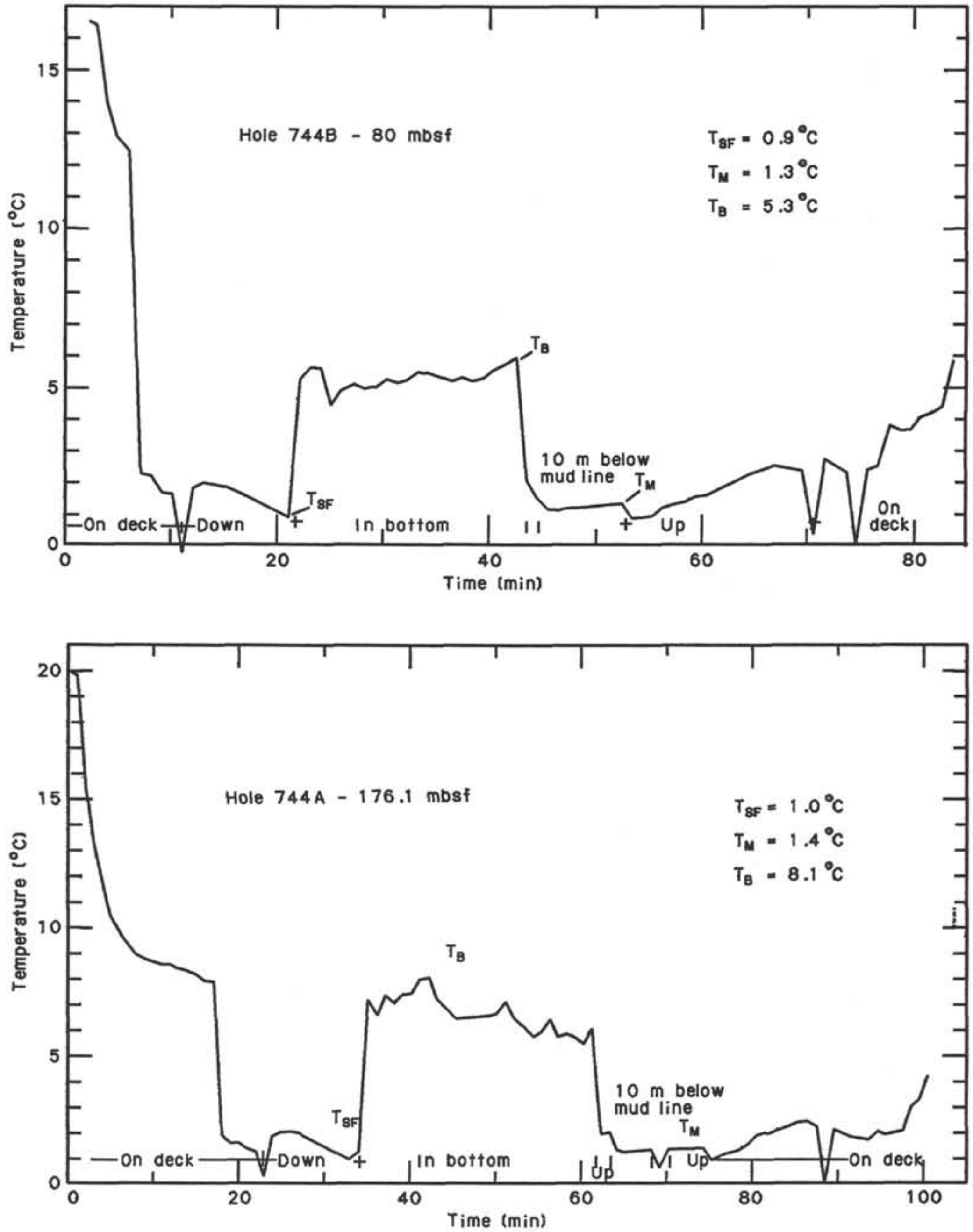

Figure 15. Temperature vs. measurement time for the two Uyeda probe deployments at Site 744 (see Table 12).

ate. This is separated by a hiatus (8.4–6.1 Ma) from 153 m of uppermost Eocene to upper Miocene nannofossil ooze. The biosiliceous content of this nannofossil ooze shows considerable variation in abundance, but it essentially disappears below the Eocene/Oligocene boundary. The detrital component at Site 744 is almost negligible.

Biostratigraphy and magnetostratigraphy indicate that the Eocene/Oligocene, Oligocene/Miocene, and possibly the Miocene/Pliocene boundaries are complete at Site 744. Hiatuses or compressed intervals occur in the middle part of the Oligocene (about 32–26 Ma), the lower Miocene (about 23–20 Ma), and in the upper Miocene (about 8.4–6.1 Ma). Southern Ocean microfossil zonations can be applied to the assemblages, but low- to middle-latitude diatom zonations can also be recognized in the upper lower Miocene and uppermost Miocene.

Lithologic Unit I is a soft diatomaceous ooze with fluctuating amounts of biogenic and calcareous sediment components. Diatoms comprise 50%–80% of this uppermost Miocene to Quaternary unit. Coarse sand grains, granules, and small pebbles up to 5 cm in diameter are disseminated throughout lithologic Unit I, ranging from <1% to 2% of the sediment in some intervals. Clasts consist of quartz, lithic fragments, granite, quartz-feldspar-biotite, gneiss, and amphibolite, and they resemble the clasts found in the diamictites of Prydz Bay. Most of the larger clasts are subrounded to subangular and are coated with black manganese oxide, commonly only on one side. These clasts are

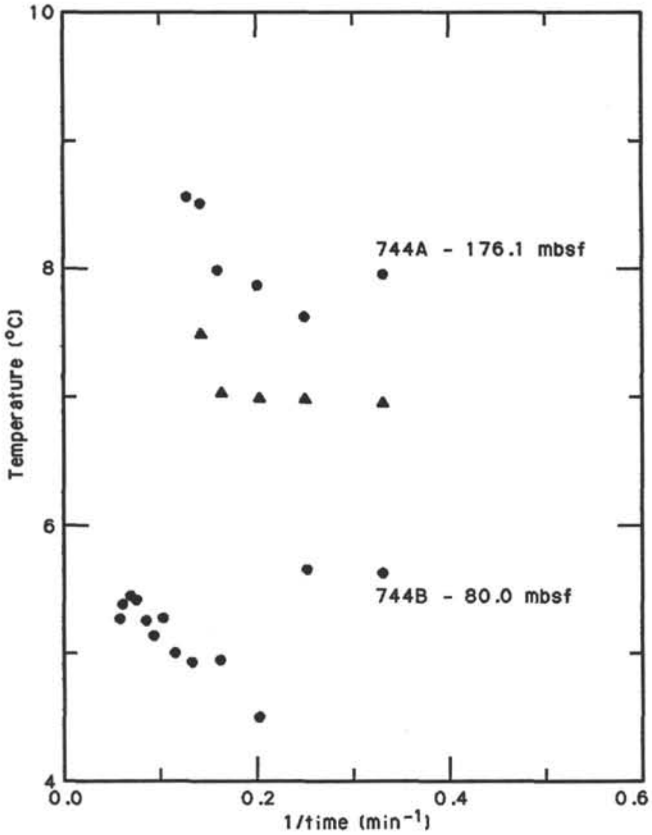

Figure 16. Temperature vs. 1/time for Uyeda-probe measurements at Site 744 (see Fig. 15 for initial penetration time and for temperature vs. time curves on which this figure is based).

most certainly ice rafted, and their occurrence in uppermost Miocene to Quaternary sediments at Site 744 mirrors their occurrence at Site 738 and probably reflects enhanced glaciation in eastern Antarctica over that of times prior to the latest Miocene.

Site 744 lies at an intermediate water depth (2307.3 m) within present-day Circumpolar Deep Water. The site probably has remained above the CCD since late Eocene time, and fluctuations in the percentage of carbonate vs. biosiliceous microfossil components probably reflect variations in surface-water fertility. The transition from nannofossil ooze to diatom ooze that occurs at the contact between lithologic Units II and I (about 23 mbsf) probably coincides with an increase in diatom productivity in the late Miocene between 8.4 and 6.1 Ma. At Site 744, this interval is marked by an unconformity, but, at Site 737 on the northern Kerguelen Plateau, this calcareous/siliceous transition occurs at 7.1 Ma, with the interval between 7.1 and 6.1 Ma (the interval removed at Site 744) represented by diatom ooze.

Calcareous nannofossils constitute >70% and mostly >80% of lithologic Unit II, the upper Eocene to upper Miocene nannofossil ooze. In the lowermost part of Hole 744A, below 147 mbsf, the carbonate component is partly disaggregated to micrite. Scattered coarse sand grains, which are probably ice rafted, are present in the uppermost part of lithologic Unit II down to Sections 119-744A-4H-3, 100 cm (27.2 mbsf), and 119-744B-4H-7 (30.8 mbsf).

In the lower part of lithologic Unit II in Section 119-744A-16H-7 and the core-catcher sample of that core (146.3–146.7 mbsf), black manganese oxide-coated, coarse sand grains (1–4 mm in diameter) are again disseminated throughout the sediment. This lower Oligocene interval was assigned to the base of magnetic polarity anomaly 13 and is, therefore, about 35.8 Ma in age, closely corresponding to the age estimate of Shackleton (1986) for the major earliest Oligocene benthic foraminiferal oxygen isotope increase (+1.0‰), which is identified globally in deep waters. Sample 119-744A-16H-CC contains a diatom assemblage (*Hemiaulus characteristicus, Hemiaulus incisus, Coscinodiscus hajosiae, Rouxia granda,* and *Stephanopyxis grunowi*) with a silicoflagellate (*Distephanus crux*) that most resembles the assemblages found in diamictites from Prydz Bay Site 739 (Cores 119-739C-25R through 119-739C-39R).

Below this lower Oligocene interval, scattered sand grains and pebbles were found in the uppermost parts of Cores 119-744A-17H (lower Oligocene) and 119-744A-20H (upper Eocene). Both of these occurrences may represent ice-rafted detritus, but the possibility of downhole contamination in the case of Core 119-744A-20H cannot completely be ruled out, as the clasts occur in soupy sediment.

Organic matter is low throughout the Site 744 sediment column, and inorganic chemistry indicates that any organic matter settling through the water column was thoroughly oxidized before it was incorporated into the sediments.

The carbonate content of lithologic Unit II is variable, and troughs of lower carbonate values (60%–70%) occur in the lower Oligocene (143.15 and 137.4 mbsf or about 35.5–34.5 Ma), middle Miocene (59.74 mbsf or about 14 Ma), upper middle Miocene (48.12 mbsf or about 11 Ma), and lower upper Miocene (37.66–37.41 mbsf or about 9 Ma), based on biostratigraphy and magnetostratigraphy. Note that with the exception of the 11-Ma interval, these intervals coincide with times of major benthic foraminiferal oxygen isotope increases, signaling the cooling of Southern Ocean waters. Such cooling probably would have caused increased biosiliceous fertility.

Physical-property measurements at Site 744 reflect the biosiliceous nature of lithologic Unit I and the nannofossil character of lithologic Unit II. Geotechnical unit G1 has index properties (water content, porosity, and bulk density) that remain fairly constant with depth, as is typical of diatomaceous sediment. A slight decrease of compressional-wave velocity occurs with depth, and a slight increase of shear strength occurs with depth in unit G1. Geotechnical unit G2 exhibits slight depth trends in response to increasing burial diagenesis; namely, water content and porosity decrease slightly with depth, while density and thermal conductivity increase slightly with depth.

REFERENCES

Barron, J. A., 1983. Latest Oligocene through early middle Miocene diatom biostratigraphy of the eastern tropical Pacific. *Mar. Micropaleontol.*, 7:487–515.

Berggren, W. A., 1972. Cenozoic biostratigraphy and paleobiography of the North Atlantic. *In* Laughton, A. S., Berggren W. A., et al., *Init. Repts. DSDP*, 12: Washington (U.S. Govt. Printing Office), 965–1001.

Berggren, W. A., Kent, D. V., Flynn, J. J., and Van Couvering, J. A., 1985. Cenozoic geochronology. *Geol. Soc. Am. Bull.*, 96:1407–1418.

Bolli, H. M., and Saunders, J. B., 1985. Oligocene to Holocene low latitude planktonic foraminifera. *In* Bolli, H. M., Saunders, J. B., and Perch-Nielsen, K. (Eds.), *Plankton Stratigraphy*: (Cambridge Univ. Press), 155–262.

Boltovskoy, E., 1978. Late Cenozoic benthonic foraminifera of the Ninteyeast Ridge (Indian Ocean). *Mar. Geol.*, 26:139–175.

Clark, S. P., 1966. Handbook of physical constants. *Geol. Soc. Am. Mem.*, 97.

Douglas, R. G., 1973. Benthonic foraminiferal biostratigraphy in the central North Pacific, Leg 17, DSDP. *In* Winterer, E. L., Ewing, J. L., et al., *Init. Repts. DSDP*, 17: Washington (U.S. Govt. Printing Office), 607–671.

Fryxell, G. A., 1988. Polymorphism in relation to environmental conditions as exemplified by clonal cultures of *Thalassiosira tumida* (Janisch) Hasle. *Proc. Int. Diatom Symp.*, 9:61–73.

Gieskes, J. M., 1983. The chemistry of interstitial waters of deep sea sediments: interpretation of deep sea drilling data. *In* Riley, J. P., and Chester, R. (Eds.), *Chemical Oceanography* (vol. 8): New York (Academic Press), 221–269.

Gombos, A. M., Jr., and Ciesielski, P. F., 1983. Late Eocene to early Miocene diatoms from the southwest Atlantic. *In* Barker, P., Dalziel, I.W.D., et al., *Init. Repts. DSDP*, 71: Washington (U.S. Govt. Printing Office), 583–634.

Jenkins, D. G., 1985. Southern and mid-latitude Paleocene to Holocene planktic foraminifera. *In* Bolli, H. M., Saunders, J. B., and Perch-Nielsen, K. (Eds.), *Plankton Stratigraphy*: Cambridge (Cambridge Univ. Press), 263–282.

Keller, G. H., and Bennett, R. H., 1971. Sediment mass physical properties—Panama Basin and northeastern Equatorial Pacific. *In* van Andel, T. H., Heath, G. R., et al., *Init. Repts. DSDP*, 16: Washington (U.S. Govt. Printing Office), 499–512.

Kennett, J. P., 1978. The development of planktonic biogeography in the Southern Ocean during the Cenozoic. *Mar. Micropaleontol.*, 3: 301–345.

Kurihara, K., and Kennett, J. P., 1985. Neogene benthic foraminifers: distribution in depth traverse, southwest Pacific. *In* Kennett, J. P., von der Borch, C. C., et al., *Init. Repts. DSDP*, 90: Washington (U.S. Govt. Printing Office), 1037–1077.

McDuff, R. E., 1978. Conservative behavior of calcium and magnesium in interstitial waters of marine sediments: identification and interpretation [Ph.D. dissert.]. Univ. of California, San Diego.

McDuff, R. E., and Gieskes, J. M. 1976. Calcium and magnesium profiles in DSDP interstitial waters: diffusion or reaction? *Earth Planet. Sci. Lett.*, 33:1–10.

Okada, H., and Bukry, D., 1980. Supplementary modification and introduction of code numbers to the low-latitude coccolith biostratigraphic zonation (Bukry, 1973; 1975). *Mar. Micropaleontol.*, 5:321–325.

Perch-Nielsen K., 1985. Silicoflagellates. *In* Bolli, H. M., Saunders, J. B., and Perch-Nielsen, K. (Eds.), *Plankton Stratigraphy*: Cambridge (Cambridge Univ. Press), 811–847.

Schnitker, D., 1979. Cenozoic deep water benthonic foraminifers, Bay of Biscay. *In* Montadert, L., Roberts, D. G., et al., *Init. Repts. DSDP*, 48: Washington (U.S. Govt. Printing Office), 377–413.

Shackleton, N. J., 1986. Paleogene stable isotope events. *Palaeogeogr., Palaeoclimatol., Palaeoecol.*, 57:91–102.

Stumm, W., and Morgan, J. J., 1981. *Aquatic Chemistry*: New York (Wiley).

Toumarkine, M., and Luterbacher, H., 1985. Paleocene and Eocene planktonic foraminifera. *In* Bolli, H. M., Saunders, J. B., and Perch-Nielsen, K. (Eds.), *Plankton Stratigraphy*: Cambridge (Cambridge Univ. Press), 87–154.

Ms 119A-112